Zeitschrift: Schweizerische mineralogische und petrographische Mitteilungen = Bulletin suisse de minéralogie et pétrographie

Band: 54 (1974)

Heft: 2-3: Alpidische Metamorphosen in den Alpen

Artikel: Metamorphic mineral assemblages in pelitic rocks of the Bergell Alps

Autor: Wenk, H.R. / Wenk, E. / Wallace, J.H.

DOI: https://doi.org/10.5169/seals-42208

Metamorphic Mineral Assemblages in Pelitic Rocks of the Bergell Alps[1])

By *H. R. Wenk**), *E. Wenk***) and *J. H. Wallace**)

With 14 figures and 10 tables in the text

Contents

Author's addresses:
* Department of Geology and Geophysics, University of California at Berkeley.
** Mineralogisch-Petrographisches Institut der Universität Basel.

[1]) Part 4 of: Geological observations in the Bergell Alps.

Abstract

The paper documents the regional distribution of sillimanite, kyanite, andalusite, cordierite, staurolite and chloritoid which are sensitive index minerals in the system Fe-Mg-Al-Si-O-H. We describe their parageneses, chemical composition and crystallographic properties and use their occurrence to derive the metamorphic evolution in this area.

The central part of the Bergell Alps from Novate to M. del Forno is characterized by an extensive *sillimanite*-zone which comprises the whole Gruf complex, most of the Bergell granite and adjacent units. Fibrolite is common and has the broader field of distribution than well-crystallized sillimanite. Textural evidence indicates that fibrolite is often a late alteration product. Sillimanite forms usually from a breakdown reaction of biotite and, more rarely, of muscovite. *Kyanite*, the typomorphic mineral of the Lepontine Alps, extends eastwards to V. della Mera. It also borders the sillimanite-zone to the north and to the south. *Andalusite* occurs to the east of the sillimanite zone in the contact area of the Bergell granite from Albigna-V. Forno-Preda Rossa. While it is the only aluminosilicate polymorph in the Murtaira-Forno region, it occurs as porphyroblasts in sillimanite- and kyanite-schists as far west as Cataeggio (to the south) and Vöga-Ciresc (to the north). In both these localities all three aluminosilicates occur in the same rock and PT-conditions must have been close to those of the triple point. *Cordierite* is common, but often difficult to identify, in the zone of highest metamorphic grade and is found mostly with sillimanite, more rarely with andalusite and kyanite. From V. della Mera eastwards cordierites become increasingly Fe-rich relative to coexisting garnets. The crystal structure of Fe_{30}-cordierite from Trubinasca was refined from X-ray diffraction data. It showed two sites for molecular water in the channel and a high likelihood for $(OH)_4$-groups in the tetrahedral framework. *Staurolite* is found within and beyond the kyanite-zone in the northern and southern belt, it is always associated with garnet. In the kyanite-zone SW of Valle della Mera (Bodengo-Liro) no staurolite is present. Staurolite displays a structural variation with orthorhombic symmetry in the low-metamorphic part and superstructured monoclinic symmetry in the area close to the sillimanite zone. *Chloritoid* is the stable Fe-aluminosilicate in the Suretta-nappe either replacing old staurolite or occurring as large bladed crystals in garnet-phyllites and chlorite-gneisses (H. R. Wenk, 1974).

The regular distribution of index minerals is an indication that equilibrium was closely approached. Therefore we use thermodynamic reasoning and experimental data for univariant reactions in the system Fe-Mg-Al-Si-O-H to estimate PT-conditions for several localities. We rely mainly on cordierite and staurolite breakdown reactions (Richardson, 1968) and reactions in the orthopyroxene-sapphirine-hercynite-cordierite-sillimanite-garnet-quartz assemblage of Codera-Bresciadega. Experimental curves for pure reactants are corrected for reactants which are diluted in mineral phases having compositions found in our specimens. PT-conditions from univariant reactions and geological constraints are consistent with an Al_2SiO_5 triple point at 5.5 kb and 625° C (Richardson et al. 1969).

On the basis of these observations a model for the metamorphic evolution in this area is suggested: Metamorphic activity started in late Cretaceous when deeply buried old rocks were subjected to anatexis and granitization. Activated by tectonic movements of the forming nappes some of this material (Bergell granite) was emplaced at high tectonic level producing a thermal aureole which is partially superposed on an older high pressure-high temperature regional metamorphism. A major event was the final emplacement of the Gruf complex from great depth (25 km). The rapid uplift of this rigid block,

undergoing an EW-tilt may be responsable for the high erosion rate W of the presently exposed Bergell granite and for the fact that pressures W of V. della Mera (Ticino) were significantly lower during the climax of metamorphism than in the Gruf complex. After these tectonic movements ended, metamorphism still lasted, evidenced by annealing features in the rock fabric and mainly by the complete recrystallization farther west which is known as Lepontine metamorphism. Thus "Alpine metamorphism" in the Bergell Alps is a sequence of events which can be separated in space and time.

INTRODUCTION

Pelitic rocks are widely distributed in many metamorphic belts. They were the first rock types to be used for defining metamorphic grade in contact zones (ROSENBUSCH 1877, Barr-Andlau, Vosges) and in regional metamorphic terrains (BARROW 1883, Scotland). But also in our century several outstanding investigations have been devoted to metamorphic pelitic rocks in many parts of the world (e. g. GOLDSCHMIDT 1920, TILLEY 1925, MIYASHIRO 1959).

In the Central Alps E. NIGGLI (1960) and E. NIGGLI and C. NIGGLI (1965) examined the regional distribution of some minerals present in aluminous schists. Based on data from literature these authors defined zones in which kyanite, sillimanite, staurolite and chloritoid occur and they outlined a central zone of high-grade Alpine metamorphism in the Canton Ticino, coinciding with the region of late- to post-tectonic partial anatexis in the southern part of the Lepontine gneiss complex (E. WENK 1956). Niggli's mineral zones are concentric to isograds of progressive regional metamorphism derived from impure calcareous-dolomitic rocks (An-content of plagioclase, E. WENK 1962; parageneses of mafic minerals, TROMMSDORFF 1966), from amphibolites (E. WENK and KELLER, 1969) and from gneisses (limit of monoclinization of alkalifeldspar, H. R. WENK 1967).

These and other investigations delineated a regular system of concentric metamorphic zones, aureoles of a crystallization which proved to be partly of equal age, but mainly younger than the planar and linear structures. Isograds derived from calcareous-dolomitic, basic, and ultramafic rocks encircle the Lepontine Alps and also include the Bergell granite and its associated country rocks to the east. But as far as pelitic metamorphic rocks are concerned, information was scanty in the region E of Ticino.

There, in the comparatively narrow sector of the Italo-Swiss Alps which is in the drainage basin of the Lake of Como and is bounded to the E by Monte della Disgrazia (see figure 1), recently a great variety of aluminosilicate minerals was found. This region comprises in Switzerland Val Bregaglia and in Italy Valle della Mera with its side valleys, and in addition Val Masino and the headwaters of Val Malenco. The area includes in its eastern part the Bergell granite with associated tonalite and metasedimentary country rocks. In its

western part it contains the prolongation of the zone of Bellinzona (part of the Lepontine gneiss complex) which dips underneath the nappe-shaped Bergell granite and reappears in the deeply entrenched window of Bagni Masino. In the northern part of the sector, N of the intercalated and still enigmatic Gruf complex, the higher Pennine nappes Tambo, Suretta and Margna are enclosed (H. R. WENK 1973, fig. 3).

The structure of these different tectonic units is complex and reflects different episodes, but it is essentially of Alpine age, as is born out by both the regular pattern of linear and planar elements in rocks of different origin and age, and by absolute age determinations. The structural reinvestigation of the Bergell Alps (H. R. WENK 1973) as well as recent studies on isotopic ages of minerals and rocks (GULSON 1973, GRÜNENFELDER et al. 1974) greatly stimulated new research on the mineral parageneses. Thus, the region outlined above and shown in figure 1, which too long has been neglected, should give valuable information on the geological history of the important border zone between the realm of regional metamorphism in the W and N, and the apparently more localized metamorphic phenomena in the marginal zones of the Bergell granite. The latter is not just a simple contact metamorphism since Bergell granite is regionally conformable, the texture is gneissose or even mylonitic and the original igneous fabric is partially recrystallized. Is this "contact metamorphism" of early explorers superimposed upon a "regional metamorphism", or does it fit into a general pattern of isograde zoning, or are the inter-relations more complex? We are well aware that within the quadrangle of 24×38 km considered (figure 1), the processes of deformation as well as those of crystallization changed in space and time, and interacted in many ways. On a regional scale, isograds are not isochrones!

The reader should also bear in mind topographic and structural elevation changes in the discussed area. For example exposures sampled in the Badile-Forno-Disgrazia group lie 2000 to 3000 m higher above sea-level than those of Valle della Mera, and there is considerable structural ascent from Valle della Mera in the W to Monte del Forno in the NE due to the easterly axial plunge (see plate 2 in H.-R. WENK, 1973), which adds to and in fact far surpasses the altimetric rise (in total 8 to 11 km corresponding to 2–3 kb). The rocks exposed in the W, in Valle della Mera, Val Codera, Val dei Ratti and Bagni Masino, record the metamorphic grade at the *base* of the Bergell granite, while those of Murtaira-Cavloccio-Monte del Forno to the NE reflect conditions of the *roof* of the granite. Thus, the reader not acquainted with the area should compare our mineral paragenetic maps with topographic maps (sheets 43 Sopra Ceneri and 44 Malojapass of the Landeskarte der Schweiz 1 : 100 000) and with the new geologic map of Switzerland 1 : 500 000. Because of this structure our working area invites a thorough study of mineral parageneses which are not only temperature but also pressure dependent. In fact, pelitic series proved

to be excellent for deriving metamorphic grade and evolution of the mineral assemblages. This is due to the large number of sensitive index minerals and assemblages which permit the evaluation of temperature-pressure conditions, and to favorable textures, indicating the relative time of crystallization. Moreover, aluminous schists are more common than calcsilicate-rocks, amphibolites and ultramafics which tend to form narrow zones and lenses, usually parallel to tectonic boundaries.

The purpose of this paper is to document the distribution of the minerals sillimanite, kyanite, andalusite, cordierite, staurolite and chloritoid in the Bergell Alps, to describe their parageneses, their chemical composition and properties, and to discuss their occurrence in terms of a metamorphic evolution. Some preliminary results from a quantitative analysis of thermodynamic implications are added. This study relies upon large collections of pelitic rocks. The authors started sampling in 1968, in a terra almost incognita, and jointly continued this exciting adventure in splendid mountain scenery until summer 1973 (only part of these last results could be incorporated in this study). We profited from a few sufficiently localized mineralogical data contained in the publications of REPOSSI (1916), CRESPI (1965), BLATTNER (1965), WEBER (1966), GYR (1967), MOTICSKA (1970), S. C. CORNELIUS (1972) and HÄNNY (1973); but the bulk of the data presented is new. As far as chloritoid, staurolite, kyanite and sillimanite are concerned, our maps may be compared with the compilation of E. NIGGLI and C. R. NIGGLI (1965), which shows in the Bergell Alps vast blank areas. But even now we are rather at the beginning than at the end of this highly interesting research on aluminosilicates. The problems are outlined, and we know of many open questions which demand further investigation.

KYANITE, SILLIMANITE AND ANDALUSITE

Selected samples of pelitic rocks containing Al_2SiO_5 polymorphs are presented in table 1. Samples which carry cordierite in addition are grouped in table 2. If in the course of our field campaigns which extended over several years duplicate specimens were gathered from the same outcrop, only the sample containing the largest number of index minerals is included in the list. The distribution maps, displayed in figures 1 and 2 of this paper, are based on the data presented in tables 1 and 2 and on the regional geological literature.

Kyanite

In the *Lepontine Alps kyanite* is the typomorphic Al_2SiO_5 polymorph of pelitic rocks in amphibolite facies. It is found as porphyroblast in schists and gneisses and as megacrysts in quartz-lenses over an area roughly 100 km long

Table 1. *Location and mineral assemblage of selected pelitic rocks containing aluminosilicates, but no cordierite. All samples contain in addition quartz*

X main constituent
O minor constituent
R relict staurolite and kyanite
F and f fibrolite

Specimen No.	Location	Coordinates	Andalusite	Sillimanite	Kyanite	Staurolite	Chloritoid	Garnet	Biotite	Muscovite	Chlorite	Epidot/Clzt	Alkali feldspar	An Plag.
Sci														
149	Castasegna	760.3/132.9				X		X	X	X	O			
153	Vec	761.4/131.8	X	X				X	X	X	X			
181	Denc dal Luf	762.6/131.4		X				X	O	X				28-33
278	Vaninetti	763.7/129.9		X					O	X	O			38-50
423	Bondo	762.0/133.2		X		X		X	X	X	O			28-30
447	Vöga	761.8/132.5		F		X		X	X	X				40-45
491	Albigna	770.6/136.2		F					X	O	O		X	
501	Murtaira	773.0/136.9		X					X	O	O			33-36
529	Cugnal	769.2/134.9		X					X		X	O	X	27-33
548	Cavloc	774.4/139.3	X					X	X	X	O			
602	Lav. Crusch	772.9/138.1		X				X	X	O				41-48
623	Codera	762.0/128.5		X	O			X	X	X				
640	Piz Cam	767.7/137.0					X	X		X	X			Ab
653	Averta	763.4/126.2		F					X	X	X	O		28-29
705	Cataeggio	tunnel	X	f	X	X		X	X	X		O		30-40
761	Vec	761.6/131.6		X	O				X	X				29-30
767	Luvartigh	763.4/132.5		F		X		X	X	X	O			29
770	Prä Salis	760.8/132.6	X	f	O	O		X	X	X			O	30-35
775	Bagni Masino	767.0/123.8		F					X	X	O			24-25
787	Ceresola	767.6/118.3		f	O			X	X	X	O	O		21-27
828	Villa	758.2/133.5				X		X	X	X	X			
874	Acqua Fraggia	755.1/136.2				R	X	X	X	X	X			Ab
877	" "	755.8/136.9				R	X	X	X	X	X			Ab
907	Muretto	776.4/135.2	X					X	X	X	X	X		26-29
909	Forno	776.1/134.4	X					X	X	O				
922	Aurosina	757.0/129.2	X					X	X		O		O	24-25
969	Sissone	776.5/130.5		f				X	X	X	O			
1001	Beleniga	755.8/128.0		X				X	X				X	
1077	Vöga	762.1/132.6		f		X		X	X	X	O			25-27
1111	L. dei Rossi	775.6/136.5	X							X				
1113	Piuro	754.2/133.1				X		X	X	X	X			
1123	Prasgnola	758.8/136.9					X	X		X	X			Ab
1141	Cambun	761.2/136.8					X	X		X	X			Ab
1154	Gudrana	758.6/131.8		F	X	X			X	X	O			
1156	Scalotta	758.7/132.4				X		X	X	X	O	X		
1158	Leira	758.4/136.2			R	R	X	X	X	X				
1161	Turbine	756.7/136.2				R	X	O		X	X			
1166	Cma di Lago	756.0/137.2				R	X	X		X	X			
1175	Angeloga	750.6/140.8			R	R		X	X	X	O			Ab
1183	P. Stella	752.5/138.5				R								
1210	Roncaiola	757.0/131.8		F		O		X	X	X	O			29-37
1213	M. Congen	758.4/130.4		X				X	X	X			X	29-37
1219	Calones	746.4/132.2				X		X	X	X				20-24
1223	Fariolo	745.5/132.0			O	X	O	X	X	X	X			
1268	Bergalgapass	762.8/138.9					X			X	X			Ab
1302	Corte Terza	742.1/125.6		f	X				X	X	O		O	
1314	Barzena	746.6/126.9			X	O		X	X	O				23-29
1316	Stabiello	752.0/118.5		F				X	X	O				25-28
1336	Naravedur	766.8/132.2		X					X	O				20-23
Brg														
65	P. Salacina	773.2/138.8	X					X	X	X				
87	P. dei Rossi	776.0/135.3	X					X	X	X	O			
94	Vöga	761.8/132.6		f	X	X		X	X	X	O			29-40
105	Cavloc	774.9/138.1	X					X	X	X	O			
129	V. dei Rossi	775.4/135.8	X	f				X	X	X	O		O	21-45
141	Piuro	754.7/132.1		X				X	X				X	27-36
146	Borgo Nuovo	753.8/133.1				O		X	X	X	X			
Mas														
30a	Cataeggio	tunnel	X	X	X	X		X	X					35-50
30f	"	"	X	O	X	X		X	X		O			40-46
32a	Sasso Bisolo	773.4/121.5		X					X	X				28-33
35a	Preda Rossa	775.2/122.5		X					X	X				35-38
45b	Baite Motale	770.1/119.8	X	O	X	X		X	X	O				35-43
46f	Cornolo	768.4/118.9		X	X	X		X	X	O				38-47
Mera														
37	M. Orso	752.7/126.7		O				X	X				X	25-33
40h	M. Peschiera	753.2/120.1		F					X	X			O	20-22
49	V. Schisone	753.2/129.0		X				X	X	O			X	28-36
50b	V. Lobbia	753.6/124.2		X				X	X					41-48
51a	V. Mengasca	749.2/124.6		F	X				X	O			X	17-21
62a	Coloredo	747.9/130.2			X	X		X	X	X	O			24-35
64a	V. Pisotta	boulder		X					X	X			O	0-4
69	Peledo	750.9/116.7		X				X	X				O	20-21
74a	T. Scarione	753.4/126.4		X				X	X	X	O			30-43
Bod														
11b	V. Garzelli	745.6/125.9		F	X			X	X	O				27-41

Table 2. *Location, mineral assemblage, chemical and optical data of selected samples of cordierite-rocks. All samples contain in addition quartz*

X main constituent F and f Fibrolite $mg = \frac{MgO}{MgO+FeO}$ mol-%
O minor constituent

Specimen No.	Location	Coordinates	Andalusite	Sillimanite	Kyanite	Staurolite	Garnet	Orthopyroxene	Sapphirine	Spinel	Corundum	Biotit	Muscovite	Chlorite	Alkali Feldspar	An Plagioklase	2V Cord.	mg Cord.	mg Biotit	mg Garnet	mg Hypersthene	mg Rock
Sci 552	P. Murtaira	773.2/137.9	X				X					X	X			40-48	76	55-59	43	15		32
Brg 104	"	773.8/138.1	X	f			X					X	X									
Sci 510	Cma. Murtaira	773.0/136.9	X	f			X			O		X	O		X	21-25						
Brg 130	P. dei Rossi	775.8/136.0	X				X					X	X			18-25	74	58	43			
Sci 1344	V. d. Largh	771.2/136.5	X	X			X					X			X	20-28						
Sci 1132	Albigna	770.1/135.7	X	O			X					X	O	O								
Sci 1230	Preda Rossa	776.8/124.6	X	X				X				X	O		O	27-43	67					
Sci 900	Cma. Murtaira	773.8/136.9		F								X	X			20-23						
Sci 1104	Mte. Rosso	775.1/132.2		X			X					X		O		29-38	77	62	45	15		
Sci 965	Vazzeda	776.9/131.6		X								X	O									
Mal 57d	V.Disgrazia	777/129		X								X				70	82-86	47-56				
Mal 57g	"	ibidem		O			X			O	O	X	O		X	60-70	78	67-71				
Mas 51a	Preda Rossa	777.0/124.7		X								X	O	O	X	21-27	81-82	71-72	57-59			
Mas 52f	"	776.5/124.1		F								X	O	O	O	23-29	80-81					
Sci 1228	"	776.3/124.1		O				X				X			O	30-40	76					
Sci 1236	Rif. Ponti	775.7/124.0						X				X			O	31-38	74-76	68	49		47	
Sci 1351	Motta Fäga	771.2/136.4		X			X					X		O		28-48						
Sci 497	V.d'Albigna	770.1/135.7		X			X					X	O			30-40	77-81	54-62				
Sci 1075	"	ibidem		X			X					X	O	O		45-65		53	46	12		
Sci 511	Spazzacaldera	768.6/134.7		X								X	O	O		30-38						
Sci 1321	Drögh	768.0/133.8		F								X			O	24-29	81					
Sci 1330	"	767.9/133.5		X								X		O		25-36	78	58	42			
Mas 50a	Bagni Masino	766.0/124.0		X			X					X				38-42	71	71	47			41
Brg 50	Lera Sura	762.6/131.8										X	X	O		23-27	74-75	93	85			90
Sci 400	Trubinasca	764.3/130.2		X								X	O	O	O		81-82	68-75				
Sci 1018	"	ibidem		X								X	O		X			67				54
Sci 1019	Vaninetti	764.0/129.5		f								X	O	O		31-43	71	78	59			
Cod 6a	V. Conco	761.7/128.0		O			X	X	X	O		X			X	25-29						
Cod 23	"	ibidem		X				X				X				33-38						
Cod 13a	V. Piana	760.6/127.3		O								X	X	O		33-35						
Sci 820	"	760.7/127.2		f				X		O		X			O	36-41		83	71		66	
Cod 18c	Mte. Gruf	759.3/126.5		O				X				X	O									
Cod 12	Bresciadega	761.1/125.4		O			X	X	X	O	O	X			X	35-40	78	86	77	51		76
Sil 17	Frasnedo	759.4/119.2		X						O	O	X	O			27-47	76-79	77-79				
Mera 65f	S. Giorgio	757.0/120.4		X								X			O	21-28	74					
Brg 43b	V. Schisone	752.7/129.2		O			X			O		X				38-45			76			
Mera 48b	"	753.1/128.9		X								X	O				76-77	94	89			91
Mera 36a	V. Trebecca	752.1/125.8		X			X					X				35-42						
Bl 523	Bodengo	745/126			O	O	O					X		O				74-79	61	29	Staur. 30-33	
	CT. Ticino:																					
Vz 691	V. Redorta	701.4/135.3			X							X		O		28-33	70-74	79-84	78			73
Vz 721a	V. Osola	701/129			X	O	X					X		X		17-20		76	61-64	29	27	56

Samples Sci: collection H.R. Wenk, Berkeley
Samples Brg, Cod, Mal, Mas, Mera and Vz: collection E. Wenk, Basel

Specimen Sci 1182b, part of a new series of sections, is a biotite-muscovite-plagioclase gneiss with large "folded" crystals of cordierite and andalusite porphyroblasts from Plotio in Val Bondasca (763.7/132.5), an extension of Lera Sura (Brg 50) zone to the north.

Errors: Specimens Sci 1228 and 1236 contain andalusite and not orthopyroxene.

(E-W) and up to 40 km broad. This vast kyanite-zone extends eastward as far as Valle della Mera, in the western part of our map. Between Gordona (4 km SW of Chiavenna) and Lago di Mezzola the alluvial plain of this valley forms its eastern border. In the pelitic rocks between Tambo-nappe and Gruf-complex, exposed in the S-slope of V. Bregaglia the kyanite-zone extends as far

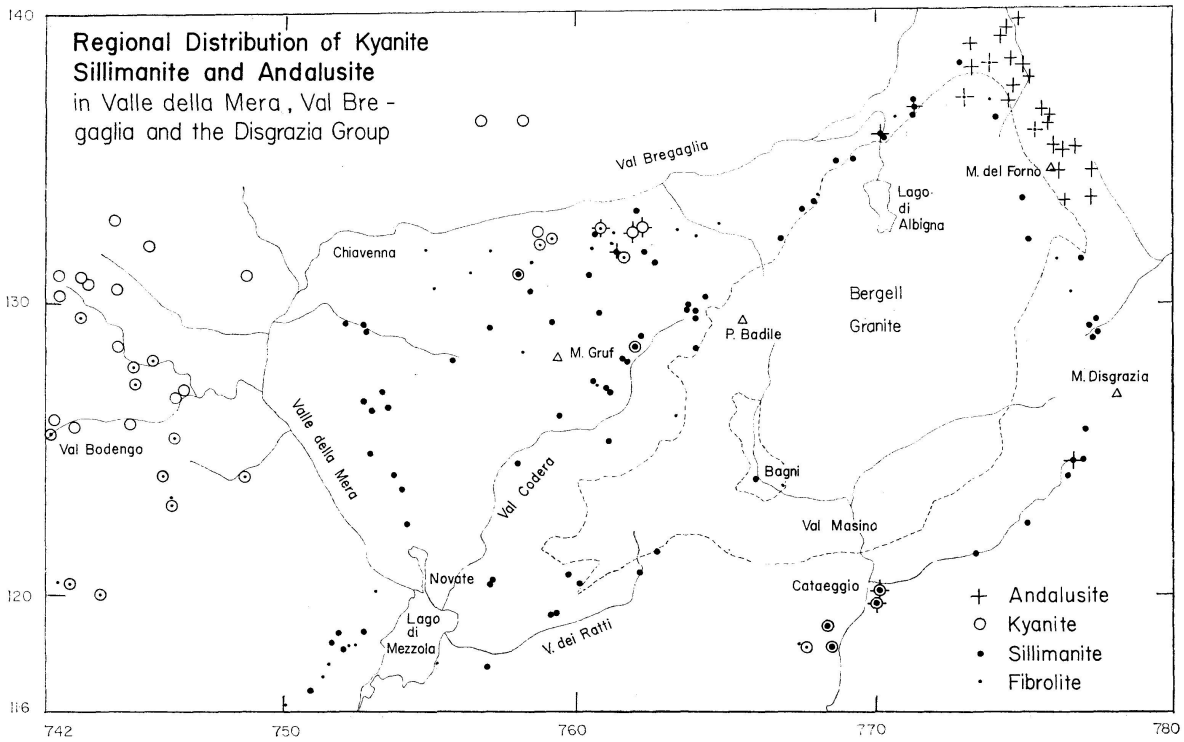

Fig. 1. Regional distribution of kyanite, sillimanite and andalusite in Valle della Mera, Val Bregaglia and the Disgrazia group. ~1:300000, Swiss km-coordinates.

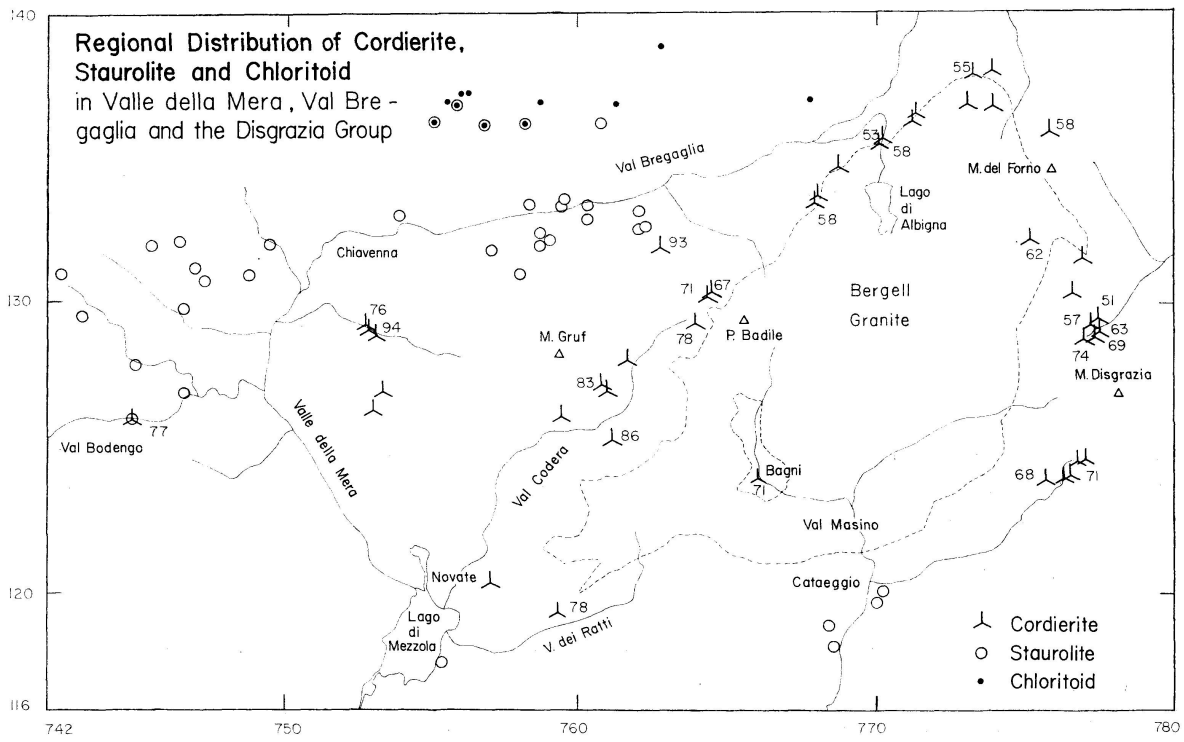

Fig. 2. Regional distribution of cordierite, staurolite and chloritoid in Valle della Mera, Val Bregaglia and the Disgrazia group. Numbers indicate mg-content of cordierite.

as Bondo although it is not documented between Mese-Calones and Sta. Croce. In addition kyanite rocks have been found recently in Val Masino in the southern part of the map. It is also here, near Cataeggio, that rocks with all three Al_2SiO_5 polymorphs have been collected. The terrain between these highly interesting sillimanite-andalusite-kyanite-staurolite-garnet-biotite-gneisses and the so called "root-zone" in the W, is unexplored. Between the northern and southern kyanite belt sillimanite is the stable aluminosilicate polymorph.

As mentioned above, the greater part of the kyanite-zone of the Central Alps is exposed in the Canton Ticino. There, kyanite is proven in several metamorphic series: in pelitic rocks associated with pyroxene-labradorite-amphibolites as well as in those alterating with oligoclase-amphibolites. The outer limit of rock-forming kyanite remains within the oligoclase-amphibolite-zone and nowhere reaches the albite-amphibolite zone (E. WENK and KELLER 1969).

Kyanite is associated with staurolite in Val Bregaglia and in the northwestern part of our map, with the latter mineral often predominating. This is in agreement with observations made in the Ticino area. But, as HÄNNY (1972, p. 54) mentioned, staurolite gets sparse and finally disappears in Val Bodengo, in the southern, higher grade members of the same pelitic series, while kyanite persists. In this zone, large megacrysts ($\sim$10 cm) of blue kyanite have been collected (Barzeno-Bodengo, Sci 1313). In the anatectic gneisses in the core of the broad Bodengo-antiform, and in the southern, vortex-structured veined gneisses of the zone of Bellinzona, both the kyanite rocks and also common biotite-plagioclase-gneisses contain *fibrolite* and, more rarely, well crystallized needles of sillimanite or sillimanite-nodules. However, a direct reaction relationship between kyanite and fibrolite is never observed. Rather they are normally separated by other mineral phases. Kyanite is typically idiomorphic or hypidiomorphic and either shows no obvious alteration or, more rarely, reaction rims of muscovite (Sci 1302, figure 3a). Fibrolite is normally associated with biotite and seems to be forming as an alteration product of it (same specimen, figure 3b). Therefore it is likely that the major metamorphic recrystallization of these specimens took place under pressure and temperature conditions where kyanite it the stable Al_2SiO_5 polymorph. Fibrolite may have formed during a subsequent partial recrystallization of the rocks under conditions favoring this new phase. If this is correct, the normally observed lack of alteration of kyanite would indicate that the reactions involving the breakdown of this mineral proceeded at a slower rate than those involving the formation of fibrolite. Sillimanite needles as accessories are even reported from cross-cutting pegmatites which postdate the main phase of crystallization. Within the kyanite zone the first occurrence of fibrolite or of accessory sillimanite is difficult to assess; it appears to start at the edge of the kyanite-staurolite-zone. The intricate problems of the fibrolite-infested kyanite-zone

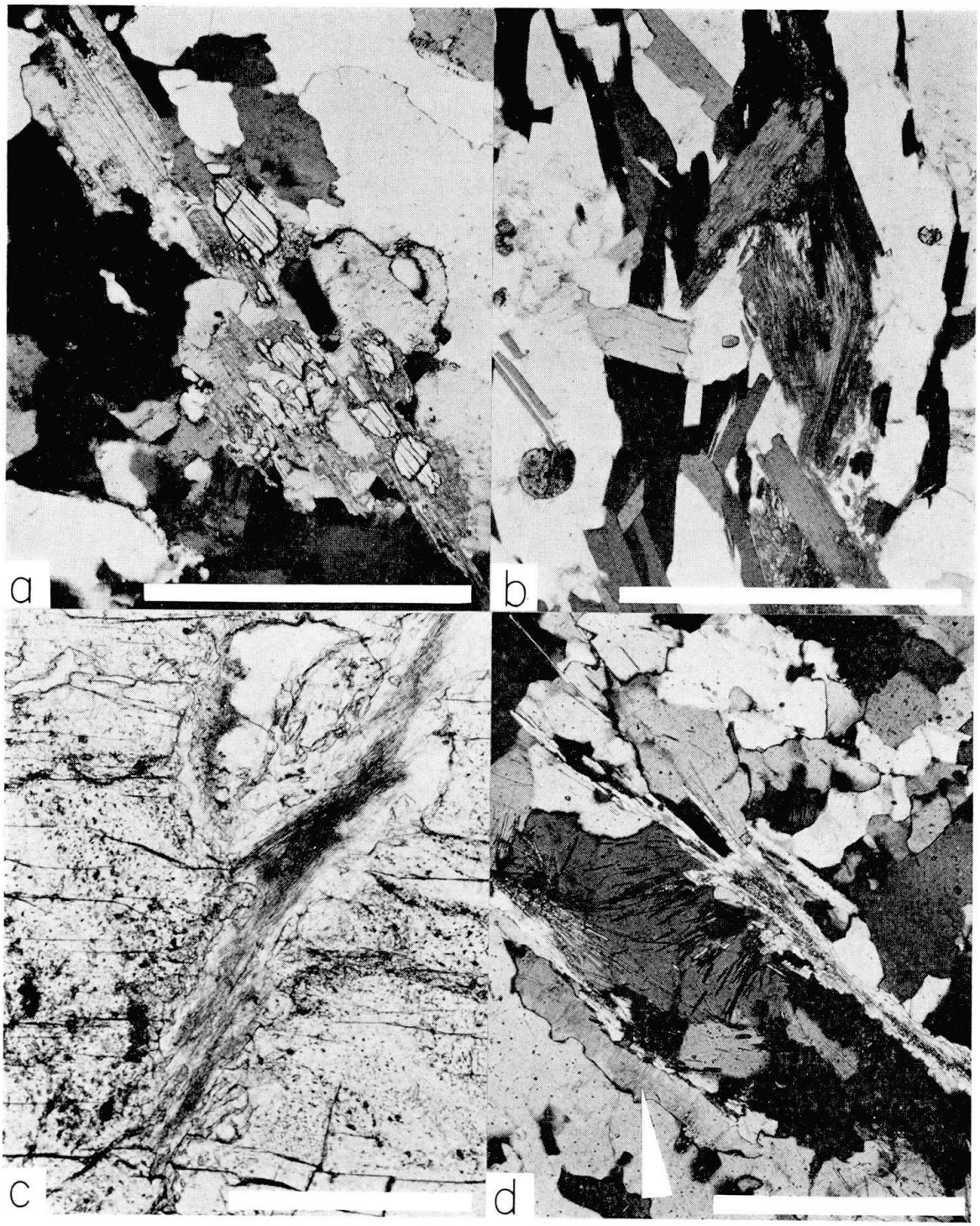

Fig. 3. Photo micrographs of selected thin sections. Bar for a and b is 1 mm, for c and d 0.5 mm.

a) Sci 1302 Corte Terza, Bodengo. Kyanite megacryst, partially replaced by muscovite. Crossed polarizers.

b) Sci 1302 Corte Terza, Bodengo. Biotite aggregate, transforming to fibrolite. Plane polarizers.

c) Sci 1078 Vöga. Fibrolite crystallizing on shear plane in an andalusite megacryst. Quartz lense. Plane polarizers.

d) Sci 626 V. Forno. Muscovite (relics) breaking down to sillimanite (needles) and K-spar (e. g. arrow). Crossed polarizers.

will be discussed in a later paper on aluminosilicates of the Lepontine Alps. We argue that this rock series cannot be regarded as belonging to a "sillimanite-zone", which really exists farther E. Table 1 gives information about the mineral association of representative rocks of the kyanite-zone.

Sillimanite

Well crystallized, prismatic *sillimanite*, which gives excellent conoscopic interference figures in sections perpendicular to the z-axis, is of common occurrence in the central region represented in figure 1. Fibrolite may also be present, but is in many cases clearly related to late shear planes, an occurrence which has also been noticed in rocks containing kyanite and andalusite (figure 3c). Tables 1 and 2 inform about the mineral parageneses. In addition to biotite, muscovite, plagioclase and garnet, the minerals cordierite and hypersthene are common, spinel, sapphirine and corundum are rare, though characteristic associates, and potash feldspar is more common than in the kyanite-zone. REPOSSI (1916) was the first scientist to draw attention to these high grade, granulite-like gneisses and compared them – not quite correctly – with those of the "zona diorito-kinzigitica" and the "stronalites" of the western Alps. Later generations of geologists plainly overlooked the occurrences of granular sillimanite in a broad zone of the Alps, and this may be responsible for the misleading representation of the "sillimanite-zone" in the compilations of E. NIGGLI (1960) and E. NIGGLI and C. R. NIGGLI (1965). A true sillimanite-zone, with characteristic mineral assemblages, and except for one single find (Sci 623, V. Codera) deprived of kyanite, extends from Valle della Mera as far as 25 km to Forno Glacier and Monte Disgrazia. It indicates eastward decreasing pressure and rising temperature.

The sillimanite-zone commences in the W at great distance from the Bergell-granite and comprises the entire gneiss series from Gruf-complex (N) to V. dei Ratti (S) which form the base of the nappe of granite. In the NE the zone reaches the tectonically much higher metasediments at the roof of the granite, which may be part of the Suretta-nappe.

Sillimanite is usually the breakdown product of micas and only in rare instances of other aluminosilicate polymorphs. As has been shown by CARMICHAEL (1969) aluminosilicate reactions are sluggish and kinetics are unfavorable. It is surprising that by far the most common reaction involves biotite. Muscovite occurs in most of the rocks, even high metamorphic members and the breakdown reaction of muscovite and quartz into sillimanite and K-spar (EVANS, 1965) has only been observed in a few cases such as in the Gruf migmatites where sillimanite is associated with perthite (Sci 1001) or in quartzite contact rocks in Val Forno (Sci 626, figure 3d). Muscovite appears on the whole as a very stable mineral.

Andalusite

In the NE the sillimanite-zone is bordered by an andalusite-zone (for parageneses see tables 1 and 2). Up to 5 cm long and often idiomorphic porphyroblasts of andalusite are found in phyllites and micaschists near the contact with the Bergell granite. The andalusite prisms show either irregular, "garben"-like (see fig. 21 in GYR 1967), or parallel orientation, with the z-axis in direction of the lineation and fold-axis of the rock. In sections cut perpendicular to the fold-axis andalusite porphyroblasts enclose folded biotite-arcs, and indicate late crystallization of andalusite. The mineral occurs also as xenoblast in micaschists of the same series and in hornfelsic gneisses and aluminous schists enclosed in the granite. This andalusite-zone, displayed in the NE-corner of figure 1, is proven to reach as far as Albigna in V. Bregaglia (Sci 1132)[2]) and on the Italian side as far as Preda Rossa (Sci 1230), or even to the occurrences in Val Masino (Cataeggio, Sci 705). These andalusite-kyanite-sillimanite rocks are described in the next section.

In the lower reaches of Val Bregaglia, in the area of Bondo-Vöga-Ciresc-Castasegna, andalusite is found in a different environment. Here in only rare cases is it observed as rock-forming mineral (Sci 770); but occurs instead as purple megacrysts in quartz-lenses and -veins of mesocratic gneisses, bearing staurolite, kyanite and fibrolite/sillimanite in their matrix. Andalusite, along with quartz and muscovite, crystallized in a late-metamorphic phase, and the geothermal curve must have passed not far from the triple point Al_2SiO_5. In shear planes of these andalusite megacrysts fibrolite has been observed (figure 3c, Sci 1075) documenting that fibrolite is indeed a very late product. This mode of occurrence is similar to that observed in the central Ticino area, where large crystals of andalusite and kyanite are common in quartz-lenses of late formation, while only kyanite, never andalusite are seen in the matrix of the country-rock. The pressure appears to have decreased during the course of crystallization. Quartz lenses with pink andalusite occur at the eastern contact (Sci 1111) at the same locality where prismatic andalusite has been observed in pelitic schists.

Coexisting Aluminosilicate Polymorphs at Cataeggio

Several specimens of rocks containing all three polymorphs of Al_2SiO_5 have been collected in 1970 E of Filorera-Cataeggio in Val Masino in scree from the tunnel of the hydroelectric power plant (Sci 705, Mas 30); lateron they could be located in situ below Baite Motale (Sci 867). They belong to the metasedimentary zone Forno Glacier–W-flank of Monte Disgrazia–Preda Rossa-

[2]) Andalusite has recently been found in cordierite-bearing rocks in Val Bondasca (Sci 1182b).

Cataeggio, which forms in Val Masino the southern border of the tonalite body. Aluminous schists and gneisses, which are well lineated parallel to Alpine fold axes, predominate, with pyroxene-amphibolites, garnet-diopside-marbles and calcsilicate-felses associated.

The melanocratic matrix of characteristic members of these aluminosilicate rocks consists predominantly of biotite, staurolite and garnet; quartz, andesine, kyanite, sillimanite and iron ore are additional components. Staurolite grains are rounded, but may be idiomorphic, and occur in direct contact with biotite, kyanite, garnet, quartz and ore, the latter three minerals form also inclusions in staurolite. Granular sillimanite (0.1 to 0.2 mm) occurs in the neighborhood of larger kyanite grains and is easily overlooked unless the optic axial angle is checked.

In this dark matrix occur light colored, bluish to purplish nuclei about 1 cm in diameter. In section perpendicular to the lineation they may show square form, but more often they have spindle shape, with the elongation axis parallel to foliation and lineation of the matrix. These nuclei which megascopically look like porphyroblasts, consist in their central part essentially of kyanite crystals with minor biotite, ore and sillimanite, rare staurolite and almandine. The marginal part of the nuclei consists of andalusite that shows homogeneous extinction over a wide area and clearly represents a younger but connected

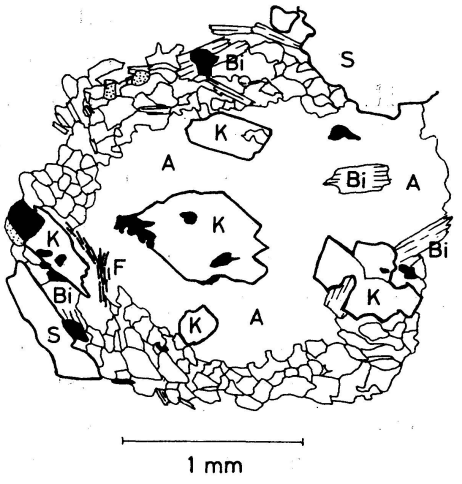

Fig. 4. Sillimanite-bearing andalusite-garnet-staurolite-kyanite-biotite-gneiss Mas 30f from Cataeggio (Val Masino). Andalusite porphyroblast enclosing kyanite, biotite and iron-ore.

stage of crystallization (see figure 4). Andalusite is separated from the biotite-staurolite-garnet-rich matrix by thin rims of fine-grained quartz and andesine. The latter are the most mobile components of the rock and form also larger spindles and layers in the matrix. Accessories of the rock are chlorite, muscovite, apatite, zircon, monazite and fibrolite which developed from biotite at a late stage of selective shearing, after the formation of andalusite.

The remarkable point at this locality is that here quite a number of samples were collected, containing all three Al_2SiO_5 polymorphs as *rock-forming* miner-

rals. Though a time sequence is noted, and andalusite, again, is slightly younger than kyanite and sillimanite, a good approach to triple point conditions is reached in these rocks. They occur in the still insufficiently explored border zone between the distribution fields of sillimanite and kyanite in Val Masino; further research may show that they are more common in this area.

CORDIERITE

Occurrence and Identification

As early as 1916 H. P. CORNELIUS (Val Codera) and REPOSSI (Val Trebecca) reported finds of cordierite in the area studied. Detailed data of the sapphirine-cordierite rock in Val Codera were given by CORNELIUS and DITTLER (1929), BARKER (1964) and MOTICSKA (1970). BLATTNER (1965), CRESPI (1965) and MOTICSKA (1970) found five new outcrops of cordierite rocks in the western and southern adjacent region, but still the mineral was thought to be rare. When we started our survey, no cordierite was known from the area N and E of the classical finds of Cornelius and Repossi, i. e. from the geologically intensively studied Val Bregaglia and the Disgrazia Group. It is mainly in this area, but also in Val Schiesone and Val Codera, that we found well over forty new outcrops of cordierite rocks and we contend that it is a fairly common but easily overlooked constituent of aluminous rocks. Preliminary information on a minor part of our collections was published by SCHWANDER and STERN (1969), H. R. WENK (1970) and E. WENK (1973).

Except for megacrysts, such as those found in Val Trubinasca and Val Codera, cordierite can only be identified by microscopic study. Refractive index, birefringence and optic axial angle alone are of little diagnostic value. Along with the very special "chagrin" of the mineral, which is hard to describe, and the wormlike pinitisation, these optical data can just give some indication. An important criterion for determinative purposes are yellow pleochroic halos around radioactive inclusions (figure 5a) which can be preserved even in pinitised grains, as MOTICSKA (1970) stated. U-stage analysis of twins and triplets, proving rhombic symmetry of the individuals is another certain means of identification (E. WENK, 1973 and figure 5b, Sci 511). Where these two criteria fail (the use of thick slides is recommended) the final identification has to be done with the microprobe. A considerable number of our proven or suspected cordierites has been tested by this method. Porphyroblasts of cordierite, such as those clear, unaltered and mostly twinned crystals of the Albigna-Murtaira or Preda Rossa area should not be mistaken for plagioclase or quartz. Because of the difficulties in identification we feel that cordierite is even more common than our map indicates. Table 2 offers a condensed list of samples, indicating their locality and mineral assemblage as well as some optical and chemical data.

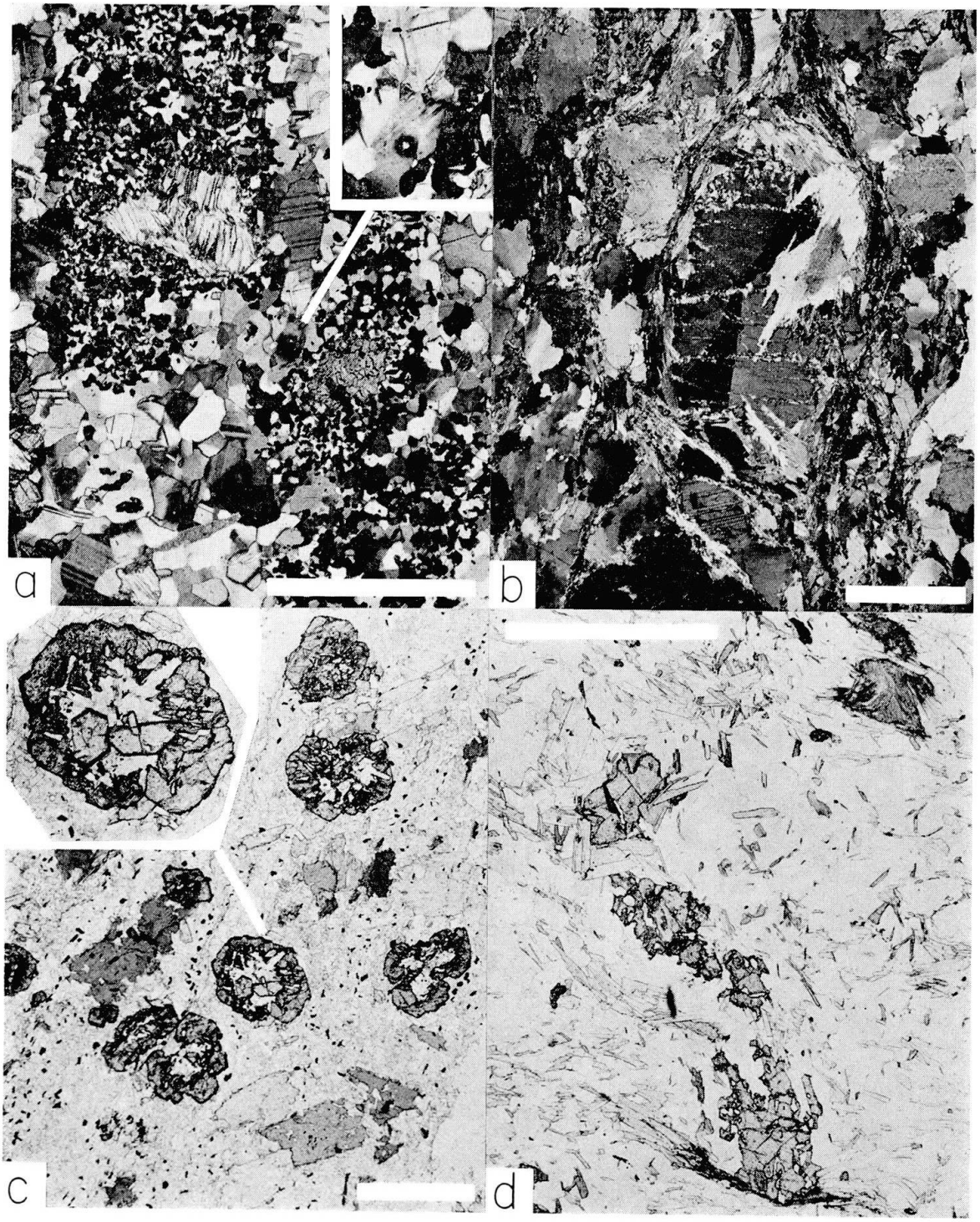

Fig. 5. Photomicrographs of selected thin sections. Bar is 1 mm.

a) Sci 820 V. Piana-Codera. Cordierite (notice halo!)-hercynite (black), hypersthene (large crystals with cleavage), plagioclase quartz aggregate. Crossed polarizers.
b) Sci 511 Murtaira. Cordierite triplet. Notice beginning pinitization. Texture indicates that the mineral crystallized before end of rock deformation. Crossed polarizers.
c) Sci 828 Villa. Euhedral crystals of staurolite growing inside garnet porphyroblast (notice enlarged portion in inset). Lower limit of staurolite stability. Plane polarizers.
d) Sci 447 Ciresc-Vöga. Skeletal crystals of staurolite from the high grade side of the staurolite stability field. Notice fibrolite aggregate at upper right corner. Plane polarizers.

Mineral Assemblage and Regional Distribution

Not one of our cordierite samples, listed in table 2, corresponds to the simple system SiO_2-Al_2O_3-MgO-FeO in bulk composition. Besides one or more of the modifications Al_2SiO_5, all of them contain biotite, plagioclase and quartz as main constituents. Andesine is the dominant plagioclase, oligoclase is common in alkalifeldspar-bearing types, labradorite confined to zones with intercalated calcareous rocks, and albite is missing. Almost half of the samples contain garnet and muscovite as a main constituent and about one third of all alkalifeldspar. Thus, K, Na, Ca and H_2O are also important components in these rocks.

In table 2 the cordierite samples are divided into three groups, beginning with andalusite assemblages, continuing with sillimanite rocks, which is the largest group and ending with the very few samples containing kyanite. Staurolite is confined to the cordierite-kyanite group and – except for the cordierite-free triple points near Cataeggio and Vöga – has not been found in andalusite rocks. Hypersthene occurs as main constituent in a quarter of all cordierite-sillimanite rocks and is here often accompanied by members of the spinel group (hercynite, gahnite), sapphirine and corundum. In these rocks cordierite is associated with hercynite in a complicated skeletal texture (figure 5a, Sci 820). Iron ores, zircon and monazite are common accessories, and the pleochroic halos produced by the latter are very useful in identifying cordierites.

Table 2 follows not only a mineralogical order, but entails also a geographical and tectonic sequence. It starts with the samples collected in the NE-corner of the map (figure 2), proceeds to the S and goes then to the W.

At a first glance the distribution scheme of cordierite may show some affinity to the pattern of the *joint* three Al_2SiO_5-modifications which reflects the course of zones of aluminous metasediments and leaves vast blank areas wherever granitic, basic or ultramafic rocks are exposed. But the occurrence of cordierite is more restricted for two reasons:

1. *Chemical composition.* The mineral is only found in those metapelitic rocks which have high Mg- and low Fe-contents.
2. *PT-conditions.* In rocks of appropriate composition cordierite is found throughout the narrow field of andalusite and the zone of well crystallized sillimanite. But our map displays only one case of a cordierite-kyanite rock (Bl. 523) – the boulder find of BLATTNER (1965). We endeavored to confirm this important occurrence by new evidence and sampled extensively in Valle Bodengo and Val Mengasca, but nowhere W of the Mera we could trace cordierite, and we conclude that it is a rare mineral in the kyanite zone. Between Chiavenna and Novate the alluvial plain of the Mera forms a distinct boundary as far as metamorphic facies is concerned. From the

western adjacent Lepontine Alps of Canton Ticino a cordierite-kyanite assemblage was reported by E. WENK (1968), but also there, in spite of extensive research, so far only one more find was made (sample Vz. 621, Osola, 1971). This is in line with experimental results indicating that the stability field of cordierite transgresses the boundary kyanite/sillimanite only in a very narrow sector (SCHREYER and SEIFERT, 1969, SEIFERT 1970, HENSEN and GREEN, 1971). From negative evidence with our samples we would also conclude, that it does not reach the triple point for Al_2SiO_5-polymorphs. The distribution pattern of cordierite is strikingly similar to that one of wollastonite in marbles. Both of them surround the northern and eastern edge of the Bergell granite, but extend in westerly direction far into the underlying gneiss and migmatite zone.

Composition and Optics

The molecular ratio $mg = \frac{MgO}{MgO + FeO}$ of cordierites from the central and western portion of figure 2 varies mainly from 0.67 to 0.79, reaching values of 0.93 and 0.94 only in Mg-rich, garnet-free and phlogopite-bearing rocks. But table 2 and fig. 2 show that mg is distinctly lower in cordierites from northern and eastern localities (0.47 to 0.62). Iron-rich cordierites occur especially in andalusite-bearing rocks of the Forno area.

We checked the problematic relation between mg and the optic axial angle of cordierite. Our data show that 2V is indeed of no diagnostic value and should be disregarded.

Crystal Structure

Cordierite from the Bergell Alps shows a *regional* distribution and at least the occurrences in the Gruf migmatites are not connected to a local contact aureole. Cooling was slow, crystallization occurred at rather high pressure and the large crystals from Alpe Trubinasca (Sci 1018) appeared to be ideal material for a structure refinement of low cordierite. We would like to briefly add crystallographic data for this relatively newly known member of Alpine metamorphic minerals. It was expected and lateron confirmed that results would closely agree with the data of GIBBS (1966) who investigated the effects of Al-Si order, but advances in analytical methods in the past years permit better resolution. The refinement of Trubinasca-cordierite is part of an investigation to determine influence of the Fe/Mg ratio on the crystal structure of low-cordierite with special view on peculiarities in thermodynamic properties of Mg- and Fe-cordierite (CURRIE, 1971; HENSEN and GREEN, 1971) and the influence of water (WOOD, 1973). For a description of the cordierite structure,

isostructural with beryl, and previous work, we refer to GIBBS (1966) and limit ourselves to a short communication of new data.

Technical procedure. A small crystal-fragment from Sci 1018, ground to a sphere (0.25 mm diameter) was selected for data collection on an automatic Picker diffractometer. Lattice constants and orientation angles were refined from the positions of 12 reflections ($a_0 =$ 17.114(3) Å, $b_0 = 9.761(1)$ Å, $c_0 = 9.331(1)$ Å). 3400 intensities were measured by the $\theta - 2\theta$ scan technique up to 2θ angles of 90° using monochromatic Mo Kα radiation with highly oriented graphite as a monochromator crystal. 2θ scan width was $2° + \Delta 2\theta$ where $\Delta 2\theta$ is the angular distance between Kα_1 and Kα_2 peaks. Scanning rate was 1° per minute with 10 sec. background counts on either side of the peak. Raw intensities were corrected for L-p effects. No absorption correction was applied ($\mu = 15$ cm^{-1}). Symmetrically equivalent reflections in space group Cccm were averaged. 2187 independent reflections with a net intensity of more than 3σ were used in the refinement. Using a local modified version of Busing-Martin-Levy's least squares program (NUCLS 6) with scattering factors from CROMER and MANN (1968) and anomalous scattering factors for Fe (CROMER, 1965) 93 positional, thermal and scale parameters (including occupancies) of 14 atoms were refined imposing proper constraints on derivatives (RAYMOND, 1972; WENK and RAYMOND, 1973). After a few cycles the refinement converged at R-values of 2.46% (unweighted) and 2.66% (weighted).

Results. Positional parameters, isotropic temperature factors (refined with atomic positions from the anisotropic model; isotropic R_1-value is 4.08%) and occupational parameters are listed in table 3 and anisotropic temperature factors in table 4. From atomic positions interatomic distances and angles have been calculated (table 5). Data compare well with GIBBS (1966) but higher resolution not only redefines structural parameters, it also poses new questions.

— Average T-O distances permit determining the Al-content of each of the five sites. Assuming the largest [T(1)] and smallest sites [T(3), T(4)] to be entirely occupied by Al, Si, respectively, one arrives at an Al-content of 8.4(2)% of the T(2) site and an Si-content of 9.0(2)% of the T(5) site. From this we calculate a total Al/Si ratio of 1.995/2.505, thus documenting a slight oversaturation in Si. The Al/Si distribution was also refined directly using occupancy factors and similar values, although with less resolution, were obtained.

— O-T-O angles show less spread for channel tetrahedra (T_3, T_4, T_5 105–114°) than for tetrahedra outside the six-membered ring (T_1, T_2 95–124°). The average angle for the former is close to the ideal value of 109.47°.

— The octahedral position is considerably distorted but the average O-Me-O angle is close to 90° (90.12°). Octahedral O-O edges which are shared with tetrahedra are significantly shorter. Me-O distances average to 2.1239 Å.

— Two channel atom-positions were refined. The position at 00 1/4 is large, very anisotropic and not well fixed (B = 13). It is occupied with an equivalent of 0.65 oxygens. The second position at 000 is spherical and shows much smaller thermal vibration (B = 2.4). The occupancy is 0.16 oxygens. GIBBS described an 000 peak in a F_{obs}-summation but attributed it to series termination errors. The improved resolution shows that this position is real.

— Temperature factors are much larger than in GIBBS' refinement. It is of particular interest that 2-coordinated oxygens O(4), O(5) and O(6) exhibit larger amplitudes of thermal vibration (B = 0.92–1.07) than 3-coordinated ones O(1), O(2) and O(3) (B = 0.72).

Table 3. *Atomic coordinates and other parameters from an anisotropic refinement of cordierite Sci. 1018*

Refinement done with half-ionized scattering factors, 2187 reflections and 93 variables. Isotropic temperature factors B refined separately. Estimated error in the least significant digit given in parentheses. $R_1 = 2.46\%$, $R_2 = 2.66\%$

Atom		Multiplier	x	y	z	B
Me	Fe	0.2782(5)	0.33733(2)	0	1/4	0.458(7)
	Mg	0.7148				
T (1)	Al	0.987(2)	1/4	1/4	0.25011(5)	0.449(8)
	Si	0				
T (2)	Al	0.01	0	1/2	1/4	0.389(10)
	Si	0.966(2)				
T (3)	Al	0.0	0.19172(2)	0.07837(4)	0	0.327(7)
	Si	0.982(2)				
T (4)	Al	0	0.13507(2)	−0.23629(4)	0	0.347(8)
	Si	0.985(2)				
T (5)	Al	0.962(2)	0.05047(2)	0.30777(4)	0	0.323(8)
	Si	0.01				
O (1)		1.017	0.24629(4)	−0.10354(7)	0.35870(7)	0.72(1)
O (2)		1.017	0.06178(4)	−0.41567(7)	0.34882(7)	0.72(1)
O (3)		1.017	−0.17317(4)	−0.30852(7)	0.35820(7)	0.71(1)
O (4)		1.017	0.04324(6)	−0.24700(11)	0	1.03(2)
O (5)		1.017	0.12142(6)	−0.18398(10)	0	1.07(2)
O (6)		1.017	0.16380(6)	−0.07885(10)	0	0.98(2)
Ch (1)	O	0.645(6)	0	0	1/4	13.1(4)
Ch (2)	O	0.163(8)	0	0	0	2.4(4)

Table 4. *Anisotropic thermal parameters of cordierite Sci. 1018*

$(\beta \times 10^5)$ {Temperature factors are of the form exp. $[-(\beta_{11}h^2+\beta_{22}k^2+\beta_{33}l^2+2\,\beta_{12}hk+2\,\beta_{13}hl+2\,\beta_{23}kl)]$}

Atom	β_{11}	β_{22}	β_{33}	β_{12}	β_{13}	β_{23}
Me	33.4(0.8)	117(3)	174(3)	0	0	−1(2)
T (1)	47(1)	121(3)	105(3)	15(1)	0	0
T (2)	31(1)	135(4)	8(5)	0	0	0
T (3)	30(1)	80(3)	102(3)	3(1)	0	0
T (4)	28(1)	95(3)	98(3)	−8(1)	0	0
T (5)	24(1)	101(3)	99(4)	7(1)	0	0
O (1)	80(2)	168(5)	178(6)	−8(2)	39(3)	−19(4)
O (2)	56(2)	238(5)	182(6)	−13(2)	5(2)	−72(5)
O (3)	65(2)	218(5)	171(6)	15(2)	−24(2)	−46(5)
O (4)	44(2)	347(10)	389(11)	−23(4)	0	0
O (5)	82(3)	248(9)	382(11)	74(4)	0	0
O (6)	97(3)	131(7)	405(11)	−42(4)	0	0
Ch (1)	3018(145)	1965(148)	1402(124)	0	0	0
Ch (2)	146(36)	340(100)	943(178)	331(50)	0	0

— No accurate chemical analysis has been available. The microprobe determination of SCHWANDER and STERN (1969) shows 30% Fe-cordierite. The best refinement was obtained with 28% Fe but a low total occupancy of the Me site indicates that the Fe content may even be lower.

— An attempt was made to refine electrostatic charges in trying to equilibrate site occupancies using proper constraints in the least squares refinement. Figure 6 is a graph showing the effect of electrostatic charge on site occupancies. It is astonishing that neutral occupancy would only be reached at more than full ionic charges which,

Table 5. *Me-O, T-O and O-O bond lengths and bond angles for cordierite Sci. 1018*
Estimated standard error in parentheses

	Me-O bond in Å		O-O bond in Å	O-Me-O angle (in degrees)
Me-octahedron				
Me-O (1)*)	2.1161(7)	O (1)–O (1)	2.8639(14)	85.17(4)
Me-O (2)*)	2.1236(7)	O (1)–O (2)*)	3.2914(11)	101.85(3)
Me-O (3)*)	2.1319(7)	O (1)–O (3)*)	2.5951(10***)	75.31(3)
		O (1)–O (3)*)	3.1925(10)	97.44(3)
		O (2)–O (2)	2.4723(14)***)	71.20(4)
		O (2)–O (3)*)	2.9088(10)	86.24(3)
		O (2)–O (3)*)	3.2998(10)	101.69(3)
average:	2.1239		2.9926	90.12
T (1) tetrahedron				
T (1)–O (1)*)	1.7547(7)	O (1)–O (1)	2.8619(13)	109.28(5)
T (1)–O (3)*)	1.7530(7)	O (1)–O (3)	2.5951(10)***)	95.44(3)
		O (1)–O (3)*)	3.1092(10)	124.85(3)
		O (3)–O (3)*)	2.8673(13)	109.73(5)
average:	1.7539		2.9017	112.31
T (2) tetrahedron				
T (2)–O (2)**)	1.6266(7)	O (2)–O (2)*)	2.4723(14)***)	98.92(5)
		O (2)–O (2)*)	2.6797(13)	110.92(5)
		O (2)–O (2)*)	2.8059(14)	119.20(5)
average:	1.6266		2.6526	109.68
T (3) tetrahedron				
T (3)–O (1)*)	1.6345(7)	O (1)–O (1)	2.6380(12)	107.57(4)
T (3)–O (5)	1.6073(10)	O (1)–O (5)*)	2.6311(11)	109.64(4)
T (3)–O (6)	1.5843(10)	O (1)–O (6)*)	2.6270(11)	108.26(3)
		O (5)–O (6)	2.6660(14)	113.30(6)
average:	1.6152		2.6367	109.45
T (4) tetrahedron				
T (4)–O (3)*)	1.6350(7)	O (3)–O (3)	2.6470(12)	108.07(4)
T (4)–O (4)	1.5750(11)	O (3)–O (4)*)	2.6563(11)	111.67(3)
T (4)–O (6)	1.6135(10)	O (3)–O (6)*)	2.6081(11)	106.81(3)
		O (4)–O (6)	2.6365(14)	111.55(6)
average:	1.6146		2.6354	109.43
T (5) tetrahedron				
T (5)–O (2)*)	1.7713(7)	O (2)–O (2)	2.8220(12)	105.61(4)
T (5)–O (4)	1.7100(11)	O (2)–O (4)*)	2.8163(11)	107.98(13)
T (5)–O (5)	1.7130(11)	O (2)–O (5)*)	2.8543(11)	109.99(3)
		O (4)–O (5)	2.8843(15)	114.84(6)
average:	1.7414		2.8413	109.40

*) Occurs twice.
**) Occurs four times.
***) Edges shared between octahedron and tetrahedron.

comparing with other silicates (WENK and RAYMOND, 1973) is unreasonable. We have at present only unsatisfactory guesses for the fact that the O-sites should have a higher electron density and the tetrahedral sites a lower one than expected from stoichiometric composition. The low occupancy of Me can be accounted for by a higher Mg/Fe ratio.

— The extinction coefficient (ZACHARIASEN, 1968) refined to $0.49(4) \times 10^{-6}$ which is of the same magnitude as in metamorphic olivines of considerable perfection.

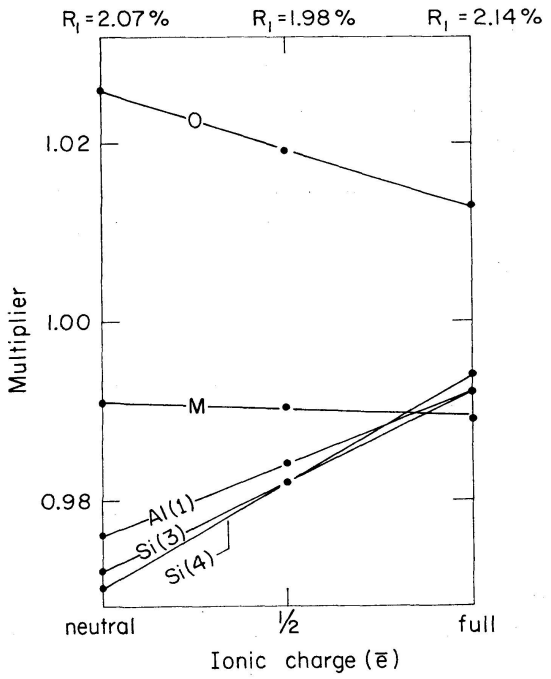

Fig. 6. Site occupancy factors of selected atoms in the structure of Trubinasca cordierite (Sci 1018) as a function of ionic charge. R_1-factors for these refinements using 1167 low-angle reflections are indicated.

An important problem which emerges from this refinement is the charge discrepancy. From past experience it seems that $^1/_{10}$–$^2/_{10}$ of the total ionic charge is a good approximation in silicates and oxides. It comes now to mind that IIYAMA (1960) suggested that some TO_4 tetrahedra may be replaced by tetrahedral $(OH)_4$ groups, a hypothesis which was later rejected by SCHREYER and YODER (1964) on the basis of evidence from infrared absorption, concluding that all water was molecular and positioned on the Ch(1) site of the channel. Charge balance could be achieved if about 0.3% of the tetrahedra were occupied by $(OH)_4$ or T-vacancies, thus indicating that (OH)-groups indeed may exist in the cordierite framework. We do not know how they are related to the Fe-content but as has been proposed by WOOD (1973) H_2O or OH may be the primary factor for variations in thermodynamic properties. To resolve this, more structure refinements and accurate chemical analyses are imperative. They were not available in time and will be given later along with crystallographic data of other Bergell cordierites of different Fe-content. In this series of determinations – for which the Bergell cordierites constitute ideal

Table 6. *Lattice constants and distortion index Δ* (MIYASHIRO, *1957*) *of Bergell cordierites*

Specimen Number	Fe/(Fe+Mg) (mole percent)	a	b (Ångströms)	c	Δ
Brg 50*)	0.07	17.083(8)	9.740(7)	9.343(4)	0.235°
Sci 624*)	0.14	17.088(3)	9.727(1)	9.335(1)	0.267°
Sci 1018*)	0.28	17.114(3)	9.761(1)	9.331(1)	0.227°
Sci 1104**)	0.38	17.06(2)	9.78(1)	9.31(1)	0.12°
Sci 552*)	0.41	17.134(4)	9.763(2)	9.328(2)	0.246°

*) Single crystal diffractometer, refined from positions of 12 reflections.
**) Precession photographs, MoKα-radiation.

material – emphasis will be on the intricate relation of Fe-content, water content, sensitive structural parameters such as electrostatic charges and the variable thermodynamic properties. Lattice constants and the distortion index Δ of some cordierites are listed in table 6. These admittedly preliminary data show no regular variation of either one of these parameters with chemical composition or regional distribution. Distortion indices spread widely in the field established for metamorphic cordierites (SCHREYER, 1966, $\Delta = 0.20$–0.29).

STAUROLITE AND CHLORITOID

In NIGGLI and NIGGLI'S distribution map the easternmost point of Alpine *staurolite* occurs in biotite schists near Verceia, probably belonging to the zone of Bellinzona (REPOSSI, 1916). Since then this mineral has been found in abundance in pelitic rocks resting on the northern limb of the Gruf anticlinorium between Chiavenna and V. Bondasca and also south of the Bergell granite near Cataeggio (figure 2). Staurolite is always associated with garnet, biotite, quartz and plagioclase, often with muscovite and clinochlor. Often it has been found together with sillimanite and fibrolite, more rarely with kyanite (Brg. 94, Sci. 1154), andalusite (Sci 770) or with all three aluminosilicate polymorphs (Sci 705, Mas 30a) at the Cataeggio locality. Nowhere in the Bergell Alps proper (E of Valle della Mera) does staurolite coexist with cordierite such as in the central Lepontine where staurolite has been found with kyanite and cordierite (BLATTNER, 1965; E. WENK, 1968) or in the Adamello where it occurs with andalusite and cordierite (JUSTIN-VISENTIN and ZANETTIN, 1968). Microprobe analyses of various staurolites show a surprisingly contant $Fe_{(total)}$ Mg ratio of 2.5 (mole) (table 8).

An interesting variation is found in Val Bregaglia. In the lower grade part (Borgonuovo-Villa-Castasegna) staurolite has a euhedral crystal form (Sci 828, figure 5c). X-ray precession photographs display only extremely weak superreflections (0kl, l = odd: DOLLASE and HOLLISTER, 1969), indicating a disordered orthorhombic structure (figure 7a). In contrast to that, staurolite coexisting with sillimanite (Vöga-Ciresc-Foppate) occurs as small skeletal crystals of irregular outline (eg. Sci 447, figure 5d). The structure of this staurolite is monoclinic with strong super-reflections, particularly 001 (figure 7b). All these staurolites are quite homogeneous and show no vector zoning. Thus they provide excellent material to study structural variations and the nature of ordering. Notice that the more highly ordered monoclinic low-entropy polymorph has been found in the area of higher metamorphic grade, suggesting that kinetic factors are important in establishing this structural variation. It is conceivable that annealing of orthorhombic staurolite could produce a superstructure.

Recently, staurolite and kyanite have been found in abundance in the

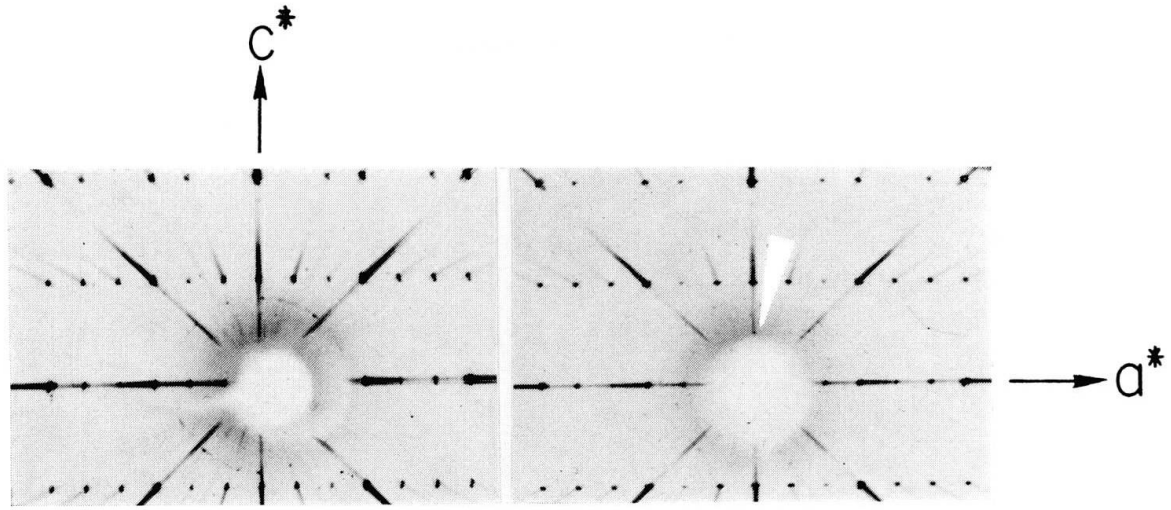

Fig. 7. Okl precession photographs of staurolite. Mo-radiation.
a) Sci 824 Villa. Notice absence of superreflections.
b) Sci 447 Vöga-Ciresc. Notice strong superreflections 1 = odd (arrow).

northern part of the Bergell Alps in rocks of the Suretta nappe belonging to the greenschist facies (H. R. WENK, 1974). Staurolite and kyanite in these rocks extending from Madesimo in the north to Vicosoprano in the south (1 km away from the Bergell granite contact) are in contrast to the above described occurrence often in large crystals which are frequently broken and partially replaced by chloritoid and mica. Nowhere in the Bergell Alps does staurolite coexist with chloritoid as in the Lucomagno (HOLST-PELLEKAN, 1913, FREY, 1969) or the Simplon area (Pizzo Teggiolo). H. R. WENK (1974) interprets Suretta staurolite as the product of a pre-Alpine metamorphic episode, most likely Caledonian (GRÜNENFELDER et al., 1974) and related to occurrences in Austro-Alpine nappes and Southern Alps. Some of these finds have been marked in the northern most part of the distribution map (figure 2).

Chloritoid, another mineral of the Fe/Mg-aluminosilicate group, is confined to the Suretta nappe where it either replaces staurolite or occurs in large bladed crystals in intensely folded garnet-phyllites. Rarely are the crystals broken in kinkfolds (Sci 1123), indicating that crystallization preceded the end of Alpine deformation. Since its occurrence is restricted to one tectonic unit, we do not feel justified at this point to use chloritoid as an index-mineral to interpret PT conditions in the Bergell Alps. Great caution is necessary in interpreting the distribution of these low grade minerals in the higher nappes across tectonic boundaries because thrust-movements succeeded at least in part their crystallization. Microprobe analyses (table 8) indicate a high iron content (26.19 weight percent FeO), but in comparison to other analyses show a considerable variation in the composition of Alpine chloritoid (e. g. FRIEDLÄNDER, 1929, V. D. PLAS et al., 1958 and FREY, 1969).

CHEMICAL COMPOSITION OF ROCKS AND MINERALS

Chemical Characteristics of Cordierite-bearing Rocks

Table 7 shows the results of 11 new chemical analyses of rocks containing Al_2SiO_5 polymorphs; five of these samples contain also cordierite. In figures 8 to 10 the analytical data published by BARKER (1964) and SCHWANDER and STERN (1969) have been incorporated as well. The AFM-diagram proposed by THOMPSON (1957) is well suited for the graphical presentation of these pelitic rocks varying considerably in composition.

Table 7. *Chemical analyses of metamorphic pelitic rocks*

(for location and mineral assemblage see Tables 1 and 2, except for Brg 134 = garnet-plagioclase-muscovite-biotite-schist from the summit of Monte del Forno, 776.0/134.45)

	Brg 134	Brg 136 = Sci 1077	Mas 30a	Mas 30b	Mas 50a	Mera 48a	Mera 51a	Mera 74a	Sci 553	Sci 1018	Vz 721
SiO_2	59.1	70.0	45.0	53.4	54.0	66.4	67.0	55.3	51.6	69.7	51.7
Al_2O_3	17.3	13.4	24.7	19.6	21.5	16.9	16.8	24.1	29.6	13.3	19.9
Fe_2O_3	0.75	0.9	2.8	4.6	1.0	0.3	1.2	0.8	1.95	0.45	1.4
FeO	8.0	4.9	11.8	7.6	9.2	1.4	5.2	8.6	6.75	4.75	8.4
MnO	0.33	0.14	0.3	0.19	0.1	0.0	0.1	0.1	0.42	0.10	0.1
MgO	4.0	2.4	5.6	4.0	4.0	9.4	2.0	2.2	2.3	3.4	6.1
CaO	4.8	1.2	2.6	2.8	1.6	0.3	0.9	0.3	0.3	1.4	1.7
Na_2O	0.8	2.0	0.7	1.8	1.5	0.5	1.6	0.6	0.9	3.0	3.4
K_2O	3.7	3.1	3.2	2.8	2.1	3.5	2.0	3.5	3.2	2.3	2.4
TiO_2	0.75	0.9	0.2	1.95	1.7	0.6	0.9	1.3	1.1	0.7	1.3
P_2O_5	0.16	0.22	0.2	0.15	0.2	0.22	0.2	0.1	0.14	0.21	0.2
H_2O^+	0.2	0.9	1.4	0.9	1.8	0.4	1.2	1.8	1.5	0.4	3.2
CO_2			0.8		0.6		0.3	0.6			
Total	99.89	100.06	99.3	99.79	99.3	99.92	99.4	99.3	99.76	99.71	99.8
Lab.	ZH	ZH	BS	ZH	BS	ZH	BS	BS	ZH	ZH	BS

Analysts: BS (Basel) W. Stern and coworkers; ZH (Zürich) M. Weibel and R. Heusser.

AFM values of rocks have been calculated in two ways and in figure 8a corresponding projections are connected by a tie-line. One of the projections (black dot) was obtained without correcting Al for Na and Ca present in the analysis; the other projection (open circle) resulted after subtraction of plagioclase from the bulk analysis. Thus the length of the tie-line indicates normative plagioclase content. The Ca-content of garnet is low and no subtraction was made for grossularite.

We notice that only those pelitic rocks contain cordierite which are high in A and M (heavy tie-line). Cordierite was not observed in iron-rich rocks with $F > 0.4$ (light tie-line). Thus the total iron content of the rock and not the Fe/Mg-ratio alone controls presence or absence of cordierite. For instance the

cordierite-andalusite schists Sci 552 and 553 from the low-pressure realm of P. Murtaira have a low Mg/Mg + Fe ratio 0.32 which is similar to many cordierite-free samples, but they are very high in A (0.48–0.54) and low in F (0.31–0.35). Of course rock types with very high Mg/Mg + Fe ratios such as samples Brg 50 (mg = 0.90) and Mera 48 (mg = 0.91) contain a Mg-rich cordierite and the coexisting tri-octahedral mica is phlogopite. Figure 8a also shows that most of the cordierite rocks are poor in feldspar, and low in Na and Ca.

Distribution of Mg and Fe on Mafic Minerals

Partial microprobe analyses of minerals are compiled in table 8. In figure 8b the AFM-projections of coexisting minerals are connected by tie-lines. This diagram shows a regular distribution pattern, dependent from rock composition (compare fig. 8a).

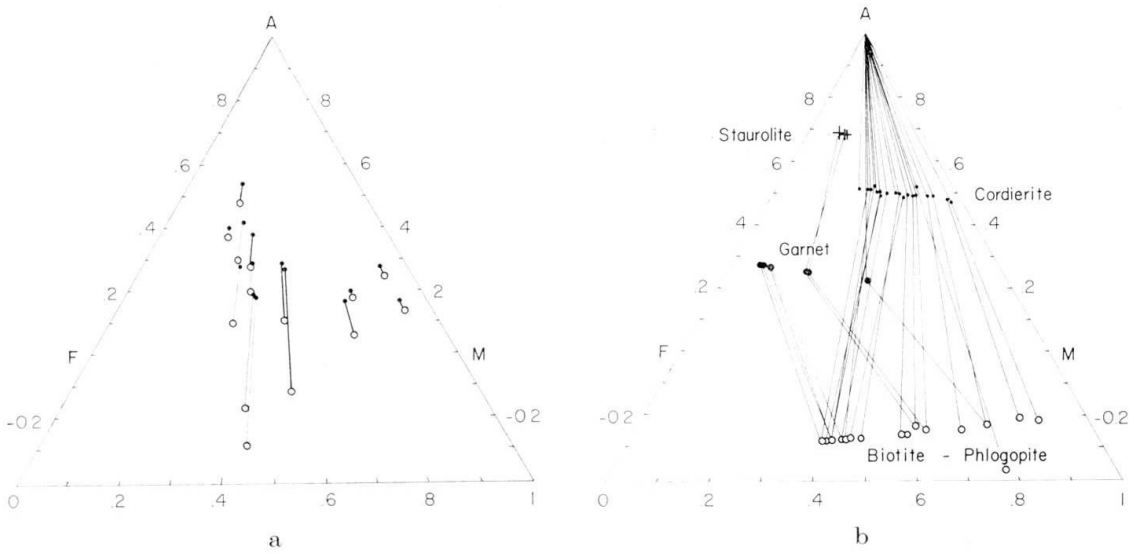

Fig. 8. AFM-diagrams.

a) Pelitic rocks (Table 7).
b) Al-rich minerals (Table 8). Coexisting minerals are connected by tie-lines.

In figure 9 the molecular ratios mg = Mg/Mg + Fe of the analyzed rocks and minerals are compared. Apart from muscovite and staurolite – minerals with restricted Fe-Mg substitution – the mg-proportion of ferromagnesian minerals is controlled by the mg-ratio of the total rock. The order of decreasing mg is clearly: cordierite > biotite ≫ garnet. This is in agreement with THOMPSON'S statement (1957, p. 857), except that staurolite can have an equal or larger mg-ratio than garnet (Cataeggio). The problem of Mg-Fe substitution in staurolite is important from the point of view of crystal chemistry as well as for the evaluation of distribution coefficients between garnets and staurolites. The Bergell Alps can provide excellent material for such a study.

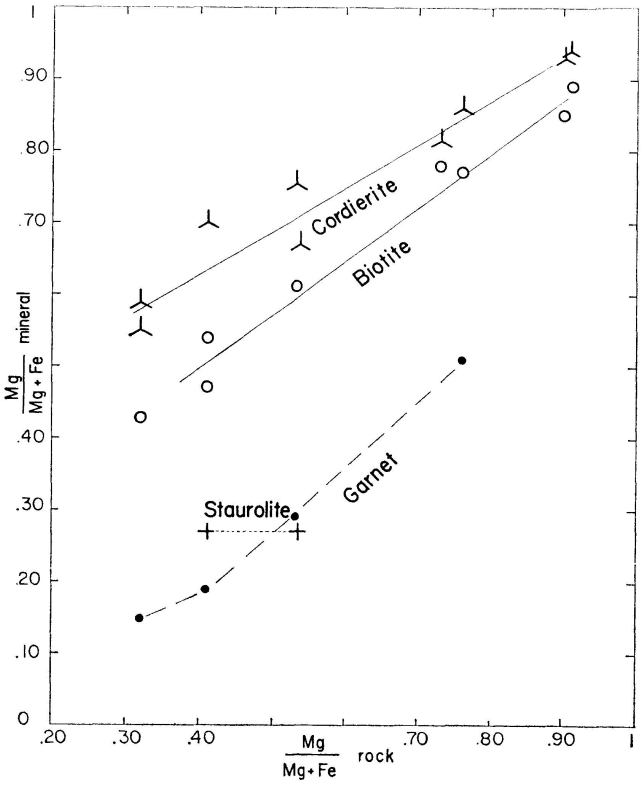

Fig. 9. mg-ratios of analyzed rocks (abscissa) and coexisting cordierite, biotite, staurolite and garnet (ordinate).

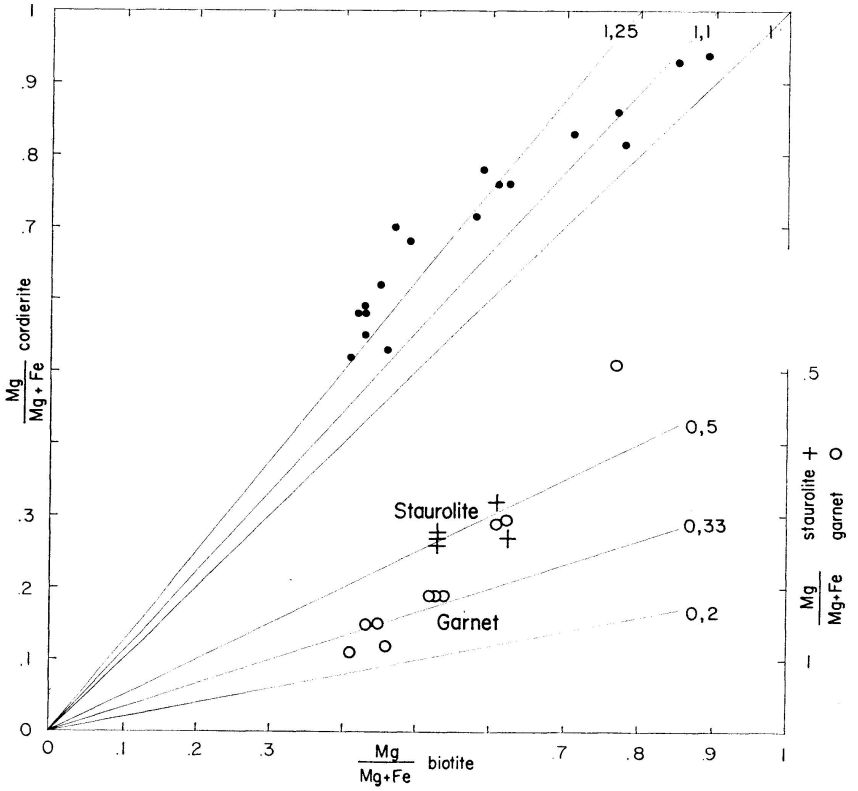

Fig. 10. mg-ratios of biotite (abscissa) and coexisting cordierite, staurolite and garnet (ordinate).

Table 8. *Partial microprobe analyses of minerals*

(weight %, Fe_{tot} as FeO, samples ordered from NE to SW)

	Sci 552	Brg 130b	Sci 909	Sci 1111	Sci 1230	Sci 770	Sci 1078	Sci 1104	Mal 57d	Mal 57g	Mas 51a	Sci 1236	Sci 497	Sci 1075	Sci 1075b	Sci 1330	Mas 50a	Sci 1018	Cod 25c	Sci 820	Sil 17	Brg 43b	Mera 48d	Mas 30f	Mas 30k	Bl 523	Vz 721a	Sci 1122
kyan. FeO																								0.3	0.2	0.5	0.3	
MgO																								0.0	0.1	0.1	0.0	
sill. FeO											0.6				0.3													
MgO											0.0				0.0													
and. FeO		0.3	0.3	0.7	1.0	0.3	0.2																	0.4	0.4			
MgO		0.0	0.0	0.0	0.1	0.1	0.0																	0.1	0.1			
cord. SiO_2	47.5	48.1															48.3	47.8					48.7					
Al_2O_3	32.6	32.8															32.2	33.0					33.4					
FeO	9.2	9.5						8.9	10.9	7.5	7.3	8.2	9.8	10.75	10.9	9.4	7.2	7.8	5.4	4.3	5.3	5.8	1.6			6.4	6.1	
MnO	0.7																0.2											
MgO	6.9	7.5						8.1	6.4	9.3	10.3	9.7	7.4	6.8	6.8	7.3	9.8	8.7	10.7	11.5	10.5	10.2	13.9			11.2	10.9	
staur. FeO																								13.3	13.9	13.6	11.8	
MgO																								2.9	2.7	3.5	2.4	
chtd. FeO																												26.2
MgO																												1.9
biot. FeO	19.7	18.8	19.9					19.0			15.6	19.1		18.6	20.2	22.3	19.3		15.7	12.5			4.6	15.9	17.3	15.4	15.0	
MgO	8.3	8.1	7.6					8.8			12.1	10.4		9.0	8.0	9.0	9.8		12.8	17.0			20.7	10.5	11.2	13.4	13.8	
garn. FeO	30.9		29.8					25.1						37.3	33.4									33.4	33.8	30.0	29.3	
MgO	3.1		1.8					2.4						2.9	2.3									4.4	4.4	6.8	6.6	
hyp. FeO												32.3								20.6								
MgO												16.1								22.1								
spin. Al_2O_3										56.4																		
FeO										24.7										33.2								
MnO										1.2																		
MgO										2.6										8.3								
ZnO										12.9																		
chlor. FeO																												29.9
MgO																												9.6
analyst	S	S	B	B	S	S	B	S	S	S	S	S	S	B	B	S	S	S	S	B	S	S	S	S	S	S	S	B

S = H. Schwander, Basel

B = C.R. Bacon, Berkeley

Cod 25c = Sci 1019

In figure 10 the mg-ratios of biotite (abscissa) and coexisting cordierite and garnet (ordinate) are compared (see also figure 8b). This diagram shows clearly that distribution coefficients vary: Projections on the left, with mg < 0.5 refer to samples from the low pressure andalusite zone (Brg 130, Sci 552), those on the upper right (Mera 48, Brg 50) to samples from the higher grade sillimanite-zone. Geothermal gradients must have changed considerably at short distance. A more quantitative evaluation of the significance of the Fe/Mg distribution in coexisting cordierite, staurolite and garnet will be attempted in the following chapter.

In Al_2SiO_5 polymorphs MgO-contents are very low and Fe is the only minor element present in clearly detectable amount (FeO 0.1–1.0). Kyanite shows lower average FeO-contents (0.3) than sillimanite and andalusite, but data are insufficient and do not permit to draw conclusions. The highest FeO-content (1.0) was determined in andalusite from Preda Rossa (Sci 1230) which shows brownish red pleochroism.

SOME THERMODYNAMIC CONSIDERATIONS

Perhaps the most fundamental aspect of the study of metamorphism is the investigation of the physico-chemical conditions under which a given mineral assemblage was formed. The purpose of this section is to evaluate and estimate some of the PT-conditions which governed the metamorphism of the Bergell Alps. We make use of experimental data and apply thermodynamic reasoning to interpret the assemblage and chemical composition of minerals in pelitic schists. Mineral assemblages are listed in tables 1 and 2, chemical analyses of minerals in table 8.

Our theoretical approach is based on several assumptions:

— It is assumed that the minerals present in a given assemblage were in a state of equilibrium at the climax of metamorphism.
— Any conclusions rely on the quality of the experimental data on which they are based.
— It is assumed that solid solutions may be treated as ideal.

If the results of the computations – using various sources of independent data – are consistent, it is an indication that not only the derived PT-conditions are correct but also that the assumptions are generally satisfied.

The basic method which we use in this chapter is to find several experimentally studied univariant reactions for the mineral assemblage in question. Whether these reactions physically took place as written and as evidenced by textural relations is unimportant as long as equilibrium existed between the reactants. Reactions on which our analysis is based are listed in table 9. These

Table 9. *Assemblage reactants were considered to be pure phases unless mole fractions are given*

1. $3\ Fe_2Al_4Si_5O_{12} = 2\ Fe_3Al_2Si_3O_{12} + 4\ Al_2SiO_5 + 5\ SiO_2$
(Fe-Cordierite) (Fe-Garnet) (Sillimanite) (Quartz)

Reference: RICHARDSON (1968)

Assemblages: 1a) Albigna $X_{Fe}^{Cord} = 0.45$ $X_{Fe_i}^{Gn} = 0.90$
1a′) Murtaira $X_{Fe}^{Cord} = 0.40$ $X_{Fe}^{Gn} = 0.85$
1a″) Monte Rosso $X_{Fe}^{Cord} = 0.40$ $X_{Fe}^{Gn} = 0.85$
1b) Val Bodengo – Ticino $X_{Fe}^{Cord} = 0.25$ $X_{Fe}^{Gn} = 0.70$
1c) Val Codera – Bresciadega $X_{Fe}^{Cord} = 0.10$ $X_{Fe}^{Gn} = 0.45$

$\Delta V = -149.02$ cc/gfw DEER et al. (1962)

2. $Fe_2Al_4Si_5O_{18} = 2\ FeAl_2O_4 + 5\ SiO_2$
(Fe-Cordierite) (Hercynite) (Quartz)

Reference: RICHARDSON (1968)

Assemblage: 2a) Val Codera – Bresciadega $X_{Fe}^{Cord} = 0.10$ $X_{Fe}^{Her} = 0.70$

$\Delta V = -38.81$ cc/gfw DEER et al. (1962)

3. $Mg_2Al_4Si_5O_{18} = Mg_2Al_4O_6(SiO_4) + 4\ SiO_2$
(Mg-Cordierite) anhydrous (Mg-Sapphirine) (Quartz)

Reference: NEWTON (1972)

Assemblage: 3a) Val Codera – Bresciadega $X_{mg}^{Cord} = 0.85$ $X_{mg}^{Sap} = 0.825$

$\Delta V = -39.13$ cc/gfw DEER et al. (1962)

4. MgAl-Orthopyroxene + Sillimanite = Sapphirine + Quartz

Reference: CHATTERJEE and SCHREYER (1972)

Assemblage: Val Codera – Bresciadega

An assemblage curve was not constructed for this reaction (see text).

5. $6\ Fe_2Al_9Si_4O_{23}(OH) + 11\ SiO_2 = 4\ Fe_3Al_2Si_3O_{12} + 23\ Al_2SiO_5 + 3\ H_2O$
(Fe-Staurolite) (Quartz) (Fe-Garnet) (Sillimanite) (Water)

Reference: RICHARDSON (1968)

Assemblages: 5a) Val Bodengo – Ticino $X_{Fe}^{Gn} = 0.70$
5b) Cataeggio $X_{Fe}^{Gn} = 0.80$

6. $Mg_2Si_2O_6 + MgAl_2SiO_6 = Mg_3Al_2Si_3O_{12}$
(Enstatite) (Al-Opx) (Mg-Garnet)

Reference: WOOD and BANNO (1973)

Assemblage: 6a) Val Codera – Bresciadega $X_{mg}^{Opx} = 0.79$ $X_{A1}^{m1\ Opx} = 0.20$ $X_{mg}^{Gn} = 0.55$

univariant curves (shown as dashed lines in figures 11 and 12) involve some mineral phases having different compositions than those found in our natural assemblages. From the experimental curves it is possible, in most cases, to construct a new univariant curve – hereafter called the assemblage curve – for the reactions as written but proceeding with reactants which are diluted in mineral phases

having compositions found in our specimens. Generally speaking, dilution of a mineral causes an increase in its stability field as compared to the pure end-member reactant of a mineral. For a given sample these assemblage curves for various reactions should, ideally, intersect at one point of a PT-diagram, representing conditions under which the assemblage equilibrated. For an accurate determination of PT-conditions it is advantageous to combine a pressure sensitive reaction (e. g. 1 in table 9) with a temperature sensitive (e. g. 5 in table 9).

At the time of preparation of this article mineral analyses were limited. We discuss four localities (Val Verzasca–Ticino–Val Bodengo, Val Codera–Bresciadega, Cataeggio, and Murtaira–Forno) and hope that similar methods can later be applied to other localities.

Curves for staurolite and cordierite reactions for all assemblages except Val Codera–Bresciadega are shown in figure 11. Val Codera–Bresciadega curves are given in figure 12. The change in volume of the reaction (Δ V) for the reaction when used is given in table 9. Volume was assumed to be constant

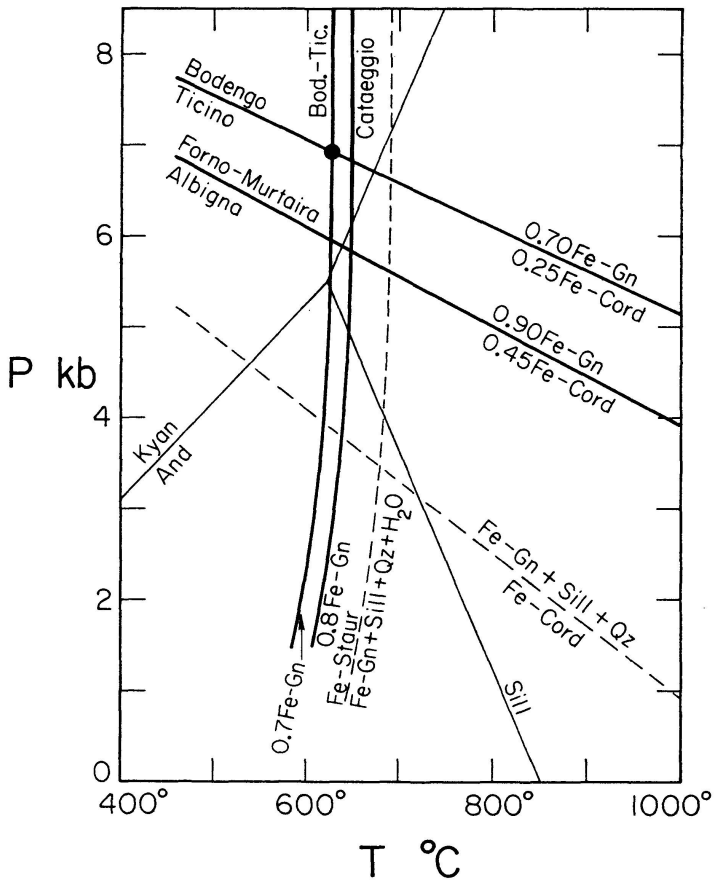

Fig. 11. PT diagram indicating equilibrium curves for univariant reactions. Dashed lines are experimentally determined curves, solid lines modified curves which correspond to mineral compositions for specific specimens.

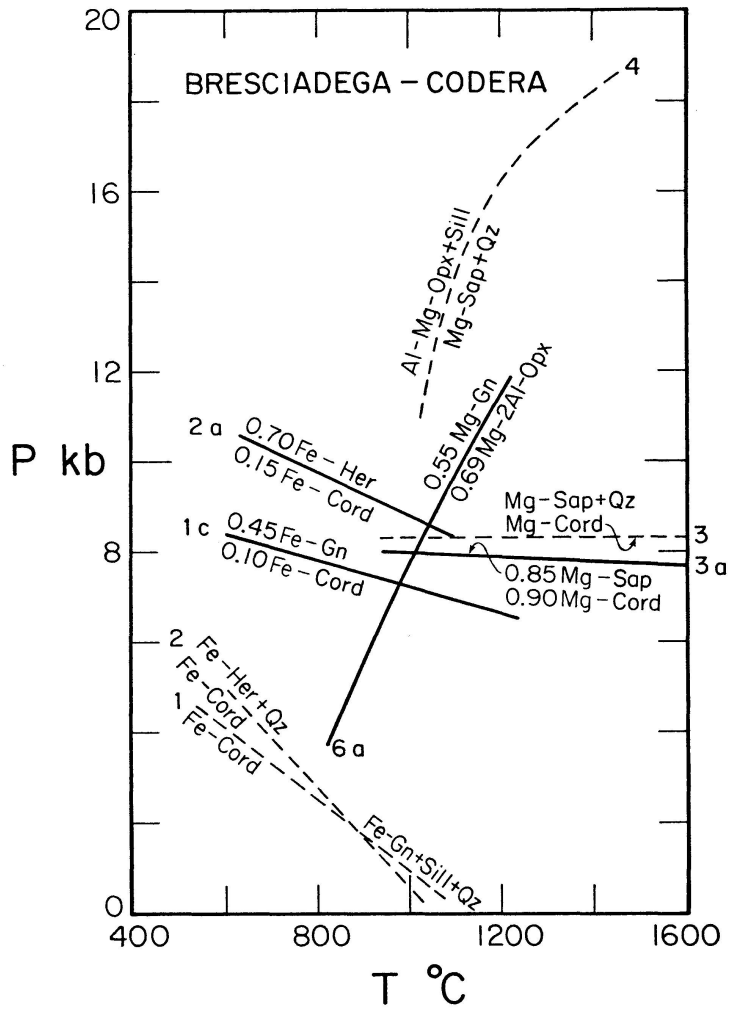

Fig. 12. PT diagram representing univariant reaction curves for sapphirine-rock from Brescia-dega-Codera. Dashed lines are experimentally determined curves, solid lines modified curves corresponding to actual mineral composition.

and equal to the value at P = 1 bar, T = 25° C. This is a fair approximation since effects of increasing temperature and pressure on volume tend to balance each other. Table 8 contains chemical analyses of minerals. For the Brescia-dega sapphirine rock data are from BAKER (1964). For other minerals only partial microprobe analyses of Fe and Mg were done. Mole fractions were calculated assuming that minerals are solutions of these endmembers only and mole functions were rounded to the nearest 0.05 value. This is not true in detail and will introduce a limited error.

Derivations

In constructing the assemblage curves for reactions 1, 2, 3 and 5 we make use of a standard reaction. This is the given reaction with all solids as pure

phases at the pressure and temperature at which the reaction is taking place and all fluids at the reaction temperature but at a pressure of 1 bar. All quantities referring either to the standard reaction or to substances at conditions in the standard reaction are denoted with the superscript ^{0}.

Reaction 1

$$\underset{\text{(Cordierite)}}{3\,Fe_2Al_4Si_5O_{18}} = \underset{\text{(Garnet)}}{2\,Fe_3Al_2Si_3O_{12}} + \underset{\text{(Sillimanite)}}{4\,Al_2SiO_5} + \underset{\text{(Quartz)}}{5\,SiO_2}$$

will be used to illustrate the method applied to construct the assemblage curves for reactions 1–3. At any point P_1, T_1 (P in bars, T in degrees Kelvin) on the experimental curve this reaction is in equilibrium when the reactants are pure phases. The thermodynamic criteria for equilibrium at constant temperature and pressure is that the Gibbs free energy change (ΔG) is equal to zero. Therefore,

$$\Delta G_{T_1,P_1} = \Delta G^0_{T_1,P_1} = 0. \tag{1}$$

The free energy change (ΔG^m) undergone by the garnet and cordierite reactants when they are mixed into general garnets and cordierites having the assemblage composition, assuming ideal mixing on two sites in the cordierite and on three sites in the garnet, is given by

$$\Delta G^m_{T_1,P_1} = R\,T_1 \ln \frac{(X^{Gn^3}_{Fe})^2}{(X^{Cord^2}_{Fe})^3} = R\,T_1 \ln \left(\frac{X^{Gn}_{Fe}}{X^{Cord}_{Fe}}\right)^6, \tag{2}$$

where X_{Fe} refers to the mole fractions of the Fe component in the given phase and R is the gas constant ($R = 82.2$ cc bar $^\circ K^{-1}$). At T_1, in order for equilibrium to be reestablished for the standard reaction, we must find some pressure (P_2) where

$$\Delta G_{T_1,P_2} = \Delta G^m_{T_1,P_2} + \Delta G^0_{T_1,P_2} = 0. \tag{3}$$

Therefore, we must change G^0 so that

$$\Delta G^0_{T_1,P_2} = -R\,T_1 \ln \left(\frac{X^{Gn}_{Fe}}{X^{Cord}_{Fe}}\right)^6. \tag{4}$$

At constant T_1

$$\frac{d\Delta G^0}{dP} = \Delta V^0,$$

where ΔV^0 is the volume change for the standard reaction. Then

$$\int_{\Delta G^0_{T_1,P_1}}^{\Delta G^0_{T_1,P_2}} d\Delta G = \int_{P_2}^{P_2} \Delta V^0\, dP.$$

Since ΔV^0 is constant and substituting for ΔG_1^0 from equation (1),

$$\Delta G^0_{T_1,P_2} - 0 = \Delta V^0 (P_2 - P_1). \tag{5}$$

Combining equation (4) and (5) and rearranging gives the final result

$$P_2 = -\frac{R T_1}{\Delta V^0} \ln \left(\frac{X^{Gn}_{Fe}}{X^{Cord}_{Fe}} \right)^6 + P_1. \tag{6}$$

This type of equation was used to construct the assemblage curves for reactions 1–3.

A different method was used for *reaction 5*

$$\underset{\text{(Staurolite)}}{6\ Fe_2Al_9Si_4O_{23}(OH)} + \underset{\text{(Quartz)}}{11\ SiO_2} = \underset{\text{(Garnet)}}{4\ Fe_3Al_2Si_3O_{12}} + \underset{\text{(Sillimanite)}}{23\ Al_2SiO_5} + 3\ H_2O$$

because it involves a fluid phase (H_2O) and because it is nearly pressure independent (see figure 11). The staurolite formula used is from RICHARDSON (1968). We assume the fugacity of oxygen is similar to that created by the quartz-fayalite-magnetite-water buffer in Richardson's experiments. Because of the lack of thermodynamic data on staurolite, several approximations had to be made. Since the entropy (S) of a fluid is normally far greater than that of a solid, and since H_2O only appears on the right side of reaction 5, we assume the total entropy change of the standard reaction at a given temperature (ΔS^0_T) to be equal to the entropy of the H_2O under standard conditions, i. e.

$$\Delta S^0_T = 3 S^0_{H_2O,T}, \tag{7}$$

where $S^0_{H_2O,T}$ is the entropy per mole of H_2O at temperature T and at a pressure of 1 bar. This number was obtained from ROBIE et al. (1968).

Since, for a mole of H_2O,

$$G_{H_2O,T,P} - G^0_{H_2O,T} = R T_1 \ln f_{H_2O,T,P},$$

where $f_{H_2O,T,P}$ is the fugacity of H_2O at T, P, at any point T, P on the experimental curve for reaction 5, assuming the pressure of H_2O is equal to the total pressure and all reactants are pure phases

$$\Delta G_{T_1,P_1} = \Delta G^0_{T_1,P_1} + R T_1 \ln f^3_{H_2O,T_1,P_1} = 0. \tag{8}$$

Therefore,

$$\Delta G^0_{T_1,P_1} = -R T_1 \ln f^3_{H_2O,T_1,P_1}. \tag{9}$$

Fugacity data for H_2O were obtained from BURNHAM et al. (1969). By substituting equations (7) and (9) into the general relationship

$$\Delta H = \Delta G + T \Delta S, \tag{10}$$

where ΔH is the heat of reaction, we find that

$$\Delta H^0_{T_1,P_1} = -R T_1 f^3_{H_2O,T_1,P_1} + 3 T_1 S^0_{H_2O,T_1}. \tag{11}$$

The free energy change of reaction 5 caused by the mixing of the garnet into a general garnet phase is given by

$$\Delta G^m = R\,T \ln (X_{Gn}^{Fe})^{12}. \tag{12}$$

At constant pressure, P_1, and at a new temperature, T_2, of equilibrium

$$\Delta G_{T_2,P_1} + \Delta G^0_{T_2,P_1} + R\,T_2 \ln f^3_{H_2O,T_2,P_1} + \Delta G^m_{T_2,P_1} = 0. \tag{13}$$

At this new temperature, from equation (10),

$$\Delta G^0_{T_2,P_1} = \Delta H^0_{T_2,P_1} - 3\,T_2 \Delta S^0_{H_2O,T_2}. \tag{14}$$

Substituting from equations (12) and (13), and solving for T_2 gives

$$T_2 = \frac{\Delta H^0_{T_2,P_1}}{3\,S^0_{H_2O,T_2} - R \ln [f^3_{H_2O,T_2,P_1} (X_{Fe}^{Gn})^{12}]}. \tag{15}$$

Assuming that ΔH^0 is constant and substituting for it from equation (11) gives the final result

$$T_2 = \frac{3\,T_1 S^0_{H_2O,T_1} - R\,T \ln f^3_{H_2O,T_1,P_1}}{3\,S^0_{H_2O,T_2} - R \ln [f^3_{H_2O,T_2,P_1} (X_{Fe}^{Gn})^{12}]}. \tag{16}$$

Since $S^0_{H_2O,T_2}$ and f_{H_2O,T_2,P_1} are both functions of T_2, equation (16) is solved through successive approximations until an estimated and a calculated value for T_2 agree.

It should be noted that there may be more water involved in reaction 5 than has been assumed, due to the uncertainty of the water content of staurolite. Additional water would cause a smaller temperature shift from the experimental curve to restore equilibrium. As the temperature shifts shown in figure 11 are rather small in the first place, it can be seen that the uncertainty introduced by an additional water content is minimal.

Reaction 6

$$\underset{\text{(Mg-Opx)}}{Mg_2Si_2O_6} + \underset{\text{(Al-Opx)}}{MgAl_2SiO_6} = \underset{\text{(Mg-Garnet)}}{Mg_3Al_2Si_3O_{12}}$$

was handled by applying the model for aluminous orthopyroxene – garnet equilibrium proposed by Wood and Banno (1973). This paper should be consulted for its derivation. Their equation for pressure as a function of temperature for the impure assemblage is:

$$P = 1 + \frac{\left[R\,T \ln \dfrac{(X_{Mg}^{M(1)})(X_{Mg}^{M(2)})^2 (X_{Al}^{M(1)})}{(X_{Mg}^{Gn})^3} + 4207 - 2.69\,T\right]}{V^0_{Mg_3Al_2Si_3O_{12}} - \bar{V}_{Mg_2Si_2O_6} - \bar{V}_{MgAl_2SiO_6}},$$

where

$X_{Mg}^{M(1)}$	is the mole fraction of Mg on the Opx M(1) site.
$X_{Al}^{M(1)}$	is the mole fraction of Al on the Opx M(1) site.
$X_{Mg}^{M(2)}$	is the mole fraction of Mg on the Opx M(2) site.
$V^0_{Mg_3Al_2Si_3O_{12}}$	is the molar volume of Mg-garnet.
$\bar{V}_{Mg_2Si_2O_6}$	is the partial molar volume of Mg-Opx in solution with Al-Opx.
$\bar{V}_{MgAl_2SiO_6}$	is the partial molar volume of Al-Opx in solution with Mg-Opx.
4207	is $-\Delta H$ for reaction 6 in calories/gfw.
2.69	is ΔS for reaction 6 in Gb/gfw.

Wood and Banno calculated values for $V^0_{Mg_3Al_2Si_3O_{12}} - \bar{V}_{Mg_2Si_2O_6} - \bar{V}_{MgAl_2SiO_6}$ for various Opx compositions. For our specimen, where $X_{Al}^{M(1)} = 0.20$, this value is -8.8 cc/gfw. The partition of Mg and Fe^{+2} between the M(1) and M(2) sites was considered by Wood and Banno to follow the experimental data of Virgo and Hafner (1969) and Saxena and Ghose (1971). On the basis of ionic radii considerations these authors assign all Ca ions to the larger M(2) site and all octohedrally coordinated Al^{+3} ions to the M(1) site. Due to uncertainty about the partition of Al^{+3} between the M(1) and tetrahedral sites, they suggest simply assigning half the total Al^{+3} to each. On a similar basis we completed the partitioning between the M(1) and M(2) sites as follows: Fe^{+3} to follow Mg, Mn to follow Fe^{+2}, and all Ti^{+4} into M(1). The ratio of Fe^{+2} to Mg on each site was considered to be the same as that determined above but their actual mole fractions on each site were recomputed to give equal total site occupancy after the Al, Ca, Ti^{+4}, Fe^{+3}, and Mn were assigned as described. Pressures were computed for several temperatures and the resulting curve is 6a on figure 12.

No assemblage curve was computed for reaction 4. Because of uncertainty about the Al content of sapphirine the exact stoichiometry and V values for this reaction are unknown. Since ΔV is small, any errors in its determination will give unacceptably large errors in the assemblage curve determination. An estimate can be made, however, if we assume that ΔV is positive. Since the dilution of the Codera orthopyroxene with respect to the experimental compositions is greater than that of sapphirine, the assemblage curve will be shifted towards lower pressures than the experimental curve. If these pressure differences are not too great, reaction 4 is consistant with the other reactions and provides a qualitative check on them.

Results

In table 10 results from these calculations are summarized and in the following paragraphs each assemblage is discussed briefly.

Table 10. *PT-limits for some pelitic assemblages*

Locality	Determinations using univariant reactions		Determinations including aluminosilicate polymorphism	
	P (kb)	T (°C)	P (kb)	T (°C)
Ticino (Verzasca)	7	630°	(7)	(630°)
Bodengo	7	630°	(7)	(630°)
Cataeggio	—	650°	6*)	645*)
Albigna	<5.8	—	~5.5*)	~700°*)
Murtaira-Forno	~5.8	—	~3.5**)	~700°**)
Bresciadega-Codera	7.5–9	1000–1100°	(7.5–9)	(1000–1100°)

*) PT for main crystallization. Andalusite porphyroblasts at lower p.
**) PT for andalusite crystallization, cordierite most likely at higher P.

Ticino (Val Verzasca) and *Val Bodengo.* The most straightfoward determinations could be done for these two localities which both have cordierite-staurolite-garnet-kyanite assemblages. The intersection of a temperature sensitive and a pressure sensitive curve determines accurately PT-conditions for the central part of the Lepontine metamorphism. The same conditions were obtained for Bodengo (Bl. 523, BLATTNER, 1969) and Verzasca (Vz 721a, E. WENK, 1968) since both assemblages have similar compositions. Minor corrections for partial pressure of O_2 and H_2O may cause small shifts. It also should be noted that both the staurolite and cordierite reactions have been determined in the sillimanite field only. The presence of kyanite will require a small correction.

Cataeggio (V. Masino, probe analyses on Mas 30 f, k). This is a three aluminosilicate assemblage with staurolite and garnet. The staurolite reaction only determines temperature but it passes very close to the triple-point (RICHARDSON et al., 1969) so the assemblage is consistent with PT of 6 Kb and 645° C during the main crystallization. (Andalusite is younger than the kyanite-sillimanite-staurolite assemblage.)

Albigna (probe analyses for Sci 1075). This assemblage contains cordierite, sillimanite and rarely late andalusite porphyroblasts. PT-conditions are estimates since no more reactions from this assemblages were used.

Murtaira-Forno. Reaction 1 has been calculated for two cordierite bearing rocks in the immediate contact zone of the Bergell granite X_{Fe}^{Gn}/X_{Fe}^{Co}-ratios for the samples Sci 552 from Murtaira (1a′) and Sci 1104 from Monte Rosso (1a″) are very similar to the Albigna sample and only a single curve is drawn in figure 11. The fact that all these andalusite-cordierite-sillimanite-garnet assemblages in the eastern contact zone from Furcelina-Vicosoprano to Disgrazia-Preda Rossa give similar X_{Fe}^{Gn}/X_{Fe}^{Co}-ratios despite different absolute iron content, is a good indication for fair equilibrium and suggests that all these rocks have undergone a very similar history. Pressure determined from cordierite-garnet is high for these andalusite schists. We attribute it to earlier crystallization of cordierite at greater depth (compare textural evidence in

figure 5b) which preceeded formation of andalusite porphyroblasts during the late emplacement.

Bresciadega-Codera. The PT-conditions for the Bresciadega-Codera assemblage have been derived from five independent univariant reactions which intersect in a limited sector of the phase diagram. Reactions 1, 3, 4 and 6 are for the Bresciadega assemblage (chemical data from BARKER, 1964), reaction 2 for nearby Val Piana (microprobe analyses for Sci 820). The determined PT is far above the minimum melt curve for granite for conditions of $P_{H_2O} = P_{total}$ (figure 13). This would indicate that P_{H_2O} was probably much less than P_{total}

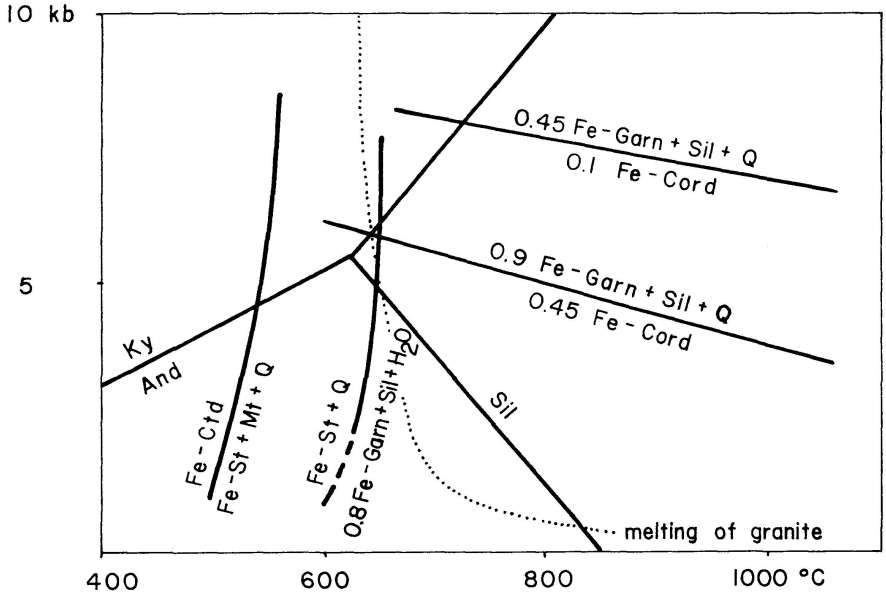

Fig. 13. PT diagram. Experimental curves are from RICHARDSON et al., 1969 (aluminosilicates), RICHARDSON, 1968 (staurolite breakdown, recalculated for 0.8 Fe-garnet which corresponds to Cataeggio; cordierite, recalculated for 0.45 Fe garnet and 0.15 Fe-cordierite, corresponding to Bresciadega-Codera and 0.9 Fe-garnet and 0.45 Fe-cordierite, corresponding to Albigna and Murtaira), GANGULY and NEWTON, 1968 (chloritoid breakdown) and LUTH et al. 1964 (minimum melting curve for granite). The figure is discussed in detail in the text.

for this assemblage which is in agreement with the low H_2O content of cordierite (ACKERMAND and SEIFERT, 1969). This justifies the use of the anhydrous reaction 3. NEWTON (1972) showed that the presence of H_2O increases the stability of cordierite in this reaction to higher pressures. Partial melting occurred in nearby migmatites and anatexis in the Novate Granite.

Conflicting data on the Mg analogue of reaction 1 (c. f. CURRIE, 1971, HENSEN and GREEN, 1971, WOOD, 1973) probably also involves the only partially understood role of water in Mg-cordierite. It is because of this conflict that the potentially useful reaction was not utilized in this paper.

Notice that the determined pressures are below values given by ACKERMAND and SEIFERT (1969) for the Bresciadega locality (12 Kb, 900° C). The very

well bracketed pressure for this Gruf complex assemblage is still higher than pressures observed in the Central Lepontine (Bodengo-Ticino).

Geological implications of these numbers will be discussed in the next section.

DISCUSSION

Mineral Parageneses and Nature of Metamorphism

The regional distribution of aluminosilicate minerals in the Bergell Alps is regular and consistent except for complications in the albite zone where an old generation of kyanite still exists and for the distribution of fibrolite which apparently often occurs as a very young alteration. It is sobering that nature is successful in establishing such a regular pattern while it is so difficult to determine stability fields of the three polymorphs in the laboratory. Also the distribution of Fe and Mg on coexisting cordierite, biotite and garnet is regular indicating that equilibrium conditions were closely approached.

The generalized figure 14 is deduced from the data contained in our tables

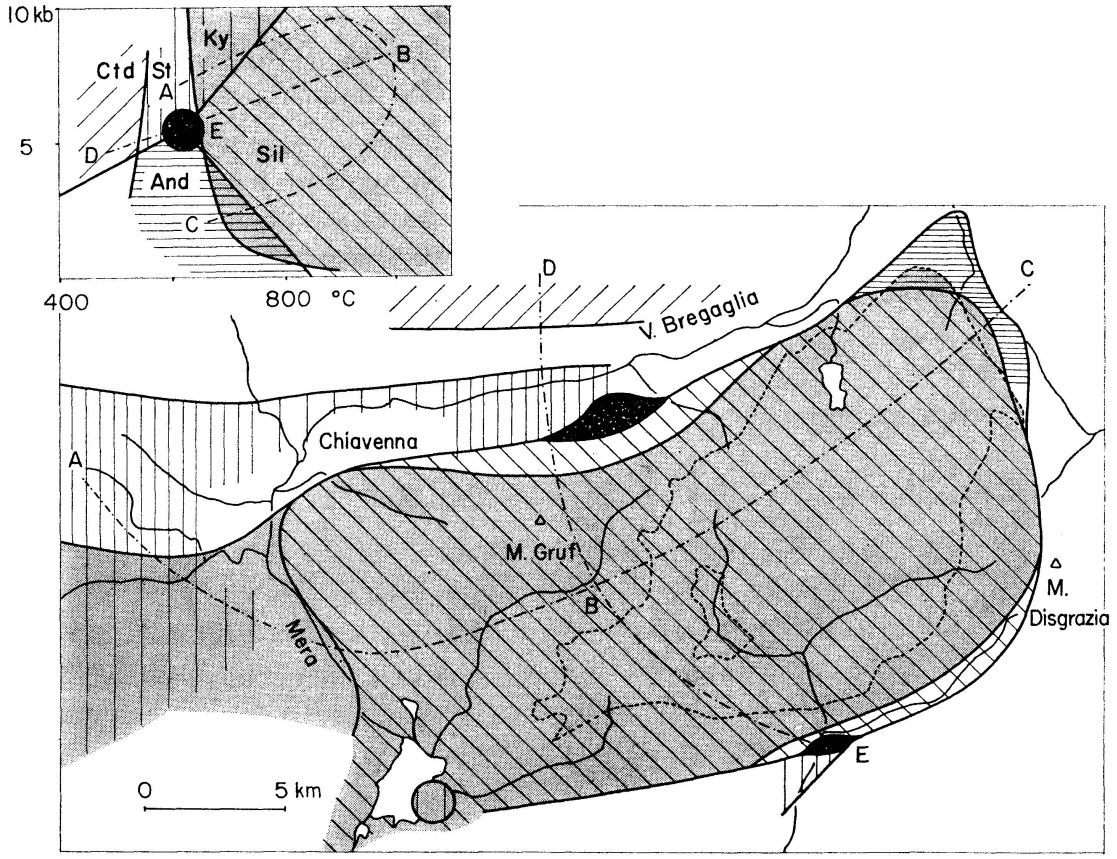

Fig. 14. Distribution of mineral assemblages of pelitic rocks and their interpretation in terms of PT-conditions (inset diagram in upper left corner, see also Fig. 13).

and maps. It shows the areal distribution of stability zones of some Al-rich silicate assemblages and the insert diagram relates them to PT-conditions[3]). Comparing the two diagrams – one based on experimental studies, the other on distribution of minerals in the field – we can evaluate their compatibility. We are strongly impressed by correlations between *observations concerned with mineral assemblages and the extent of partial anatexis.*

— Only a small part of the sillimanite zone is without anatectic phenomena. A belt about 100 m–500 m wide exists on the north side of the Bergell Alps that contains well-crystallized sillimanite but lacks anatexis (e. g. Lera Sura, Brg 50, Foppate, Sci 1152). The Al_2SiO_5 triple point of RICHARDSON et al. (1969) is close to the minimum melting curve of granite but on the low-temperature and low-pressure side, thus leaving a narrow sector of the sillimanite field outside the area of melting (LUTH et al., 1964).

— A significant portion of kyanite bearing rocks occurs in the zone of regional anatexis (e. g. Val Bodengo, zone of Bellinzona). According to the PT-diagram this is to be expected at pressures above 6 kb and temperatures above 650° C.

— "Triple-point" rocks usually contain staurolite. Staurolite is rare in the zone of anatexis and has a narrower field than kyanite. At low metamorphic grades it occurs beyond kyanite as is seen in V. Bregaglia. This is consistent with the phase diagram which displays a primarily temperature dependent staurolite zone between 550° C and 650° C which includes the triple point and shares only a small sector with the field of melting (figure 13).

— Cordierite commonly occurs in the sillimanite and the andalusite-zone, but is only rarely found in the kyanite zone. It is usually associated with partial anatexis. Cordierite was not observed in rocks near the triple point, but this may be due to rock composition. The Fe/Mg-ratio in cordierite-garnet assemblages is lowest in sillimanite-rocks of the Gruf complex and highest in andalusite-schists of the eastern contact of the Bergell granite. The phase diagram displays a large stability field for cordierite mainly limited by pressure. Unusually high pressures were derived for pelitic assemblages in Val Codera (table 10 and figure 12) and PT-conditions are well within the field of granite melting. The absence of large quantities of mobilisates can plausibly be explained by unfavorable rock composition and a very dry environment. At present we have no satisfactory answer for the wide distribution of muscovite even in these granulite facies-type rocks and the

---

[3]) For the scaling of P and T we rely strongly on experimental data of RICHARDSON (1968) and RICHARDSON et al. (1969), Of course there are uncertainties in these boundaries. We estimate them to be in the order of $\pm 50°$ C and ± 0.5 kb. We are aware that this inset diagram will have to be modified in the future.

problem of distribution, relative age and composition of muscovite in the Bergell Alps deserves further investigation. Comparing PT-conditions and assemblages we notice an inconsistency: 0.45 Fe cordierite –0.9. Fe garnet should not coexist with andalusite (e. g. Sci 1132 Albigna, also Murtaira and Forno). But textural evidence shows that andalusite, although a product of the same metamorphic event, crystallized later than most other minerals.

— Chloritoid has not been found in equilibrium with staurolite. The boundary must be somewhere in the Tambo nappe, whose granite-gneisses are of unfavorable composition to contain these minerals.

Another consideration is the implied geographic distribution of *temperature-pressure gradients*. To ease explanation, figure 14 contains lines connecting facies series in geographic space and on the PT-diagram (traces ABC and DBE). On the latter these lines are schematic, but it is apparent that temperature-pressure gradients vary considerably along these paths. The trace ABC leads from the staurolite-kyanite zone N of Bodengo (A) through the anatectic kyanite zone and sillimanite-cordierite zone (B, Bresciadega-Codera) to the andalusite-field (C). Gradients in the W are around 30°C/km. Eastwards of B, which has been located accurately at 8–9 kb (30–35 km depth) and 900°C to 1000°C, the pressure decreases rapidly at almost constant temperature. Towards C both temperature and pressure decrease first with a shallow gradient then increasingly steep reaching 70–100°C/km around C in the roof of the Bergell granite. A negative gradient of –10°C/km is documented for the trace EC. It images the transition from regional metamorphism to contact metamorphism whereby the heat-source is situated at high tectonic level. The lines DB and EB represent facies series touching the triple point. The gradient is more uniform (30–40°C/km).

A section drawn from Chiavenna eastward towards Val Bondasca, along the intermediate unit between Tambo-nappe and Gruf-complex, would offer similar conditions. Pelitic members are very common in this series. N of Chiavenna they contain only biotite, muscovite and garnet, near Borgonuovo-Castasegna staurolite comes in, at Ciresc-Vöga also fibrolite, kyanite and rarely andalusite are found. This pelitic series of the "intermediate unit" (H. R. Wenk, 1973) indicates eastward increasing temperature at moderate to high pressure and, again, a rather uniform gradient.

The variation in gradient is striking. It excludes the possibility of a simple pattern of posttectonic metamorphism. Assuming that all mineral assemblages were formed during an "Alpine metamorphism" we conclude that metamorphic isograds were influenced either by processes of magmatic intrusions (high gradients) or tectonic movements during or after crystallization (low gradients). Except for the andalusite zone of the Forno region which reflects conditions

of *contact* metamorphism at the roof of the Bergell granite, the gradients indicate *regional* metamorphism and are consistent with normal continental geothermal gradients. Local occurrences of andalusite near Cataeggio and Ciresc-Vöga also fit this latter type. There is no sharp boundary between the two regimes.

DAUBRÉE (1859), who coined the term "regional metamorphism", was well aware of the fact that different types of metamorphism can grade into each other. We quote from his original paper (p. 77): "Il résulte de tout ce qui précède, qu'il serait difficile d'établir une distinction nette entre le métamorphisme de juxtaposition (contact metamorphism) et le métamorphisme régional, en se fondant seulement sur les caractères minéralogiques: les deux phénomènes diffèrent surtout par leur étendue."

The parageneses around B in the Gruf complex can be explained by late uplift of basement rocks, crystallized at high pressure and temperature, and then juxtaposed in a lower grade environment. Nowhere in the Bergell Alps is there any evidence – so far (e. g. WENK, 1974) – for high pressure-low temperature assemblages which are commonly associated with subduction zones along plate boundaries (ERNST, 1973).

A last argument concerning figure 14 takes into account the *regional geology* and specifically the *depth of burial* of individual tectonic units as implied from field observations. A reasonable estimate can be made for the sillimanite-andalusite transition zone exposed in the Forno area (C, NE-corner of figure 14). The isograd is situated at the roof of the Bergell-granite approximately 1 km away from the thrust-contact of the Margna-nappe (H. R. WENK 1973, figure 7). H. P. CORNELIUS (1935, p. 315–316), an experienced expert, well acquainted with tectonic and petrologic aspects of the Central and Eastern Alps, is – to our knowledge – the only geologist who offered a clear statement on the thickness of the nappe-pile in this region. He calculated for the base of the Margna-nappe in uppermost Bergell valley a load of 5–6 km (1 km Margna-nappe, 4–5 km lower and upper Austroalpine elements), and regarded this figure as a reasonable, but possibly low estimate. A maximum burial of 11 km can be read from the profiles of other authors. We believe that a span of 7–10 km (2–3 kb) is correct for this boundary between the fields of sillimanite and andalusite, and for the cover of the Bergell granite. Less reliable are estimates for the triple point near Ciresc. H. R. WENK (1973, profiles on plate 3), judging from the northern, unthinned parts of the nappes, adds for the Tambo and Suretta 8 to 11 km, thus accumulating an overload of 15–20 km in the area of Ciresc. This depth of burial of three-alumino-silicate assemblages agrees reasonably with the experimentally determined triple point of 5.5 kb (RICHARDSON et at., 1969). The second author (E. W.) assumes above Ciresc, on the southside of Val Bregaglia, a considerably reduced thickness of Tambo and Suretta and favours a burial of 10–14 km (2.8–4 kb) which would be in better

agreement with HOLDAWAY (1971). The tectonic overload of the triple point at Cataeggio is more difficult to assess since the tectonic position of these rocks is uncertain and they occur in strongly deformed parts of the root-zone.

It is difficult to account for the 10–20 km (3–6 kb) pressure difference along traverses DB, CB, and EB while actual distances between points are only 10–15 km. Again we must conclude that the high pressure regime required for the mineral assemblages in the Gruf complex (e. g. Bresciadega-Codera 8–9 kb, 900–1000° C) cannot have been achieved at the present tectonic setting of this unit. Rocks were uplifted and strongly deformed after crystallization.

Geological Interpretation

With some reservation these considerations tend to affirm the validity of the phase diagram presented in figures 13 and 14, and we can now incorporate it into an interpretation of the metamorphic history of the Bergell Alps. But doing this we should keep in mind that the question of metamorphic evolution, discussed in this paper, is only one of the many puzzling problems of the Bergell granite – a granite in a regional metamorphic environment – which await further investigation. Any synthesis is preliminary and subject to change.

First there is some background information which must be taken into account:

From *structural work* (H. R. WENK, 1973) we know that crystallization of most minerals and especially the solidification of the Bergell granite preceeded the end of the thrust movements and folding in this area. This is different from the central Lepontine where crystallization often outlasted tectonic movements. Assuming a simultaneous deformation we conclude that crystallization in the Bergell preceeded the Lepontine metamorphism.

GULSON (1973), GULSON and KROGH (1973) and GRÜNENFELDER et al. (1974) determined with *radiometric dating methods* that a large part of the Bergell Alps consists of old crystalline basement which was altered during various episodes of metamorphism. Discordant U/Pb ages of zircons indicate that the most intensive phases, all accompanied by the formation of megacrystic granites, were Caledonian (Suretta and higher Pennine nappes, Austroalpine nappes and Southern Alps), Hercynian (Tambo nappe) and Tertiary (Bergell and Novate granite). An age of 30 m. y. is generally assumed for the climax of Tertiary granitic activity.

On the other hand boulders of Bergell granite and of tonalite are found abundantly in the paleontologically dated lower to middle Oligocene Molasse near Como and between Como and Varese (CITA, 1957), corresponding to 31–38 m.y. in absolute time scale. A recent K-Ar determination by JÄGER (1973) gives an age of 28 m.y. for biotite separated from these boulders. Hopefully the conflict between the stratigraphic and the isotopic age will be reduced by new paleontological data. But even so the rate of erosion must

have been extremely high to remove 6–10 km of overlying nappes above the roof of the granite in order to expose it (allowing 2 m.y. this would amount to an erosion rate of 5 mm per year). This fast erosion can only have lasted a short period since Bergell granite still exists in great thickness, indicating only modest erosion during the past 30 m.y.

These conflicts can be resolved in part if we assume that boulders of granite in the Molasse were derived from a *now eroded western part* of the granite nappe above Valle della Mera (see H. R. WENK 1973, p. 285) which may have extended over part of the Ticino culmination. Such a western source, much closer to the place of deposition, would also account for the high frequency of granite boulders in the conglomerate. Bergell granite comprises less than one percent of all presently exposed rocks in the drainage basin of Lake Como.

Using this information we attempt to come up with a model. Isotope data indicate that a long period of metamorphic activity started in late Cretaceous. At deep levels old rocks were subjected to anatexis and granitization (GRÜNENFELDER et al. 1974), possibly as part of an extensive regional metamorphism (JÄGER, 1973). Activated by tectonic movements of the forming nappes some of this granitic material (Bergell granite) was emplaced at high tectonic levels producing a thermal aureole which is partially superposed on an older high pressure-high temperature regional metamorphism. Products of this at least partially igneous activity are andalusite and cordierite bearing hornfels-type gneisses along the eastern granite contact.

Simultaneous with this recrystallization tectonic movements continued resulting in large strains in many of the units, including the Bergell granite. A major event was the final emplacement of the Gruf complex, representing deep-seated basement material, as a rigid block, undergoing an EW-tilt and thus exposing in the west extreme high pressure-high temperature assemblages. In the Bergell such rapid *vertical* movements (cf. RAMBERG, 1967) have been of major importance in the establishment of metamorphic zones as they are displayed today.

Farther west the *Lepontine* metamorphism not only outlasted the emplacement of Bergell granite and Gruf complex but also the Alpine thrust movements.

Locally in the Ticino there are similar tectonic disturbances as indicated by zones with steep fold axes and high metamorphic grade but vertical movements were never as dominant as in the Bergell Alps.

Thus we view the *emplacement* of the Bergell granite and Bergell *contact metamorphism* (Forno-Sissone-Preda Rossa) as resulting initially from igneous, later from tectonic processes. A thermal aureole was superposed as a brief episode on an extensive and lasting *regional metamorphism* which proceeded farther west (Lepontine). Such a solution seems to agree with present data and reconciles the conflicting views of GULSON (1973), E. WENK (1962) and H. R. WENK (1973), that the contact metamorphism is younger, equal in age

or older than the regional metamorphism. The earlier conclusions were based on different evidence (isotopic age, mineral assemblage, structure) from different localities.

Our experience with the Bergell Alps makes us uncomfortable with the term "Alpine metamorphism". Does it stand for metamorphism in the Alps or does it represent a specific episode in geological history? Metamorphic processes were active in many orogenies and left imprints which are still partially preserved. Even Tertiary metamorphism was a succession of episodes which are separated in time and space. We discussed in this paper the burial metamorphism of old basement, the contact metamorphism of the Bergell granite and the eastern part of the Lepontine regional metamorphism. We did not mention the Cretaceous pretectonic metamorphism documented in the Eastern Alps (JÄGER, 1973). It is obvious from this discussion that metamorphic processes cannot be evaluated separately from tectonic and structural questions. Hence we suggest analyses of the succession of metamorphic reactions in many locations in the Alpine orogenic belt. Until this tedious groundwork is done the question of *cause* for the metamorphic evolution remains debatable. Solution of this problem has not only to take into account the distribution of mineral assemblages, it should be based on a thorough understanding of the geological structure, the regional history, the stratigraphic facies of associated sedimentary rocks, and on geophysical evidence (in this respect the gravimetric studies conducted by the group in Paris, are most promising). Since we do not as yet have this information we rather conclude this presentation of data without adding uncertain speculations.

Future Work

In conclusion we wish to recall some problems which emerged in the process of this study and which seem most pressing:

— The general regional geology appears to be solved in principle, but the proposed model is by no means refined. A detailed thermodynamic analysis of mineral assemblages in associated mafic, ultramafic and carbonate rocks, along the same lines of reasoning as used in this paper, will not only help in determining PT-conditions (and also partial pressures of H_2O, O_2 and CO_2) for specific localities, it also will help in further evaluating consistency of experimental data. In pelitic schists, reactions involving biotite, muscovite and feldspar would supply further parameters to refine physicochemical conditions.

— Several phases of metamorphism have been separated. It would be desirable to have more radiometric dates in order to establish accurate time-limits for these episodes. With the present background crucial questions (e. g. Gruf) become obvious and should be solved by experimental approach.

— Some intriguing crystallographic questions emerged for which the pelitic minerals of the Bergell Alps provide excellent material. The study of the crystalchemistry of Fe-Mg cordierite seems a most attractive project. There is strong evidence that part of the water is on tetrahedral sites in the structure and this could account for thermodynamic peculiarities. Water content may have an important effect on the stability of cordierite.
— Staurolite occurs both with and without a superstructure. The monoclinic superstructure has been found in crystals formed in the vicinity of the triple point, while orthorhombic staurolite seems to be confined to lower grade rocks. The nature of the superstructure and its petrological significance deserve further investigation.

Acknowledgements

We wish to thank Ch. Bacon (Berkeley) and Prof. H. Schwander (Basel) for microprobe analyses of minerals. Prof. M. Weibel (Zürich) and Dr. W. Stern (Basel) made some of their unpublished rock analyses available. Discussions with Prof. F. J. Turner (Berkeley) on petrological problems and with Dr. B. Wood (Manchester) on geochemistry were most fruitful. We acknowledge further help from J. Fitzpatrick (microscope analyses of some specimens), J. Hampel (photomicrographs) and H. Klein (drawings). The work was partially supported by NSF grant GA 29294 (to HRW).

REFERENCES

SMPM = Schweiz. Mineral. Petrog. Mitt.

Ackermand, D. und Seifert, F. (1969): Druck und Temperaturbedingungen bei der Bildung der sapphirinführenden Gesteine von Val Codera. Fortschr. Mineral. 47, Suppl. I, 1 (abstract).

Barker, F. (1964): Sapphirine-bearing rock, Val Codera, Italy. Amer. Mineral. 49, 146–152.

Barrow, G. (1893): On an intrusion of muscovite-biotite gneiss in the south east highlands of Scotland. Geol. Soc. London quart. J. 49, 330–358.

Blattner, P. (1965): Ein anatektisches Gneissmassiv zwischen Valle Bodengo und Valle di Livo (Prov. Sondrio und Como). SMPM 45, 973–1071.

Burnham, C. W., Holloway, J. R. and Nicholas, F. D. (1969): Thermodynamic Properties of Water to 1000° C and 10,000 Bars. Geol. Soc. of Amer. Spec. Paper No. 132.

Carmichael, D. M. (1969): On the mechanism of prograde metamorphic reactions in quartz-bearing pelitic rocks. Contr. Mineral. Petrol. 20, 244–267.

Chatterjee, N. D. and Schreyer, W. (1972): The Reaction Enstatite + Sillimanite $\rightleftarrows$ Sapphirine + Quartz in the System MgO-Al_2O_3-SiO_2. Contr. Mineral. Petrol. 36, 49–62.

Cita, M. B. (1957): Studi stratigrafici sul Terziario subalpino lombardo, sintesi stratigrafica della Gonfolite. 1st Geol. Paleont. Univ. Milano, Serie G, publ. no. 97.

Cornelius, H. P. (1916): Ein alpines Vorkommen von Sapphirin. Zbl. Mineral. 11, 265–269.

— (1935): Geologie der Err-Julier-Gruppe. I. Teil: Das Baumaterial (Stratigraphie und Petrographie, excl. Quartär). Beitr. Geol. Karte Schweiz, N.F., Lfg. 70 I, 1–321.

Cornelius, H. P. and Dittler, E. (1929): Zur Kenntnis des Sapphirinvorkommens von Alpe Bresciadega in Val Codera (Italien, Prov. Sondrio). Jb. Mineral. 59, 27–64.

Cornelius, S. B. (1972): The geology of upper Val Masino. M.A. thesis, Univ. Calif. Berkeley.

Crespi, R. (1965): Migmatiti e rocce verdi di Bagni del Masino. Sci. Istituto Lombardo A 99, 685–704.

Cromer, D. T. (1965): Anomalous dispersion corrections computed from self-consistent field relativistic Dirac-Slater wave functions. Acta Cryst. A 18, 17–23.

Cromer, D. T. and Mann, J. B. (1968): X-ray scattering factors computed from numerical Hartree-Fock wave functions. Acta Cryst. A 24, 321–324.

Currie, K. L. (1971): The reaction 3 cordierite = 2 garnet + 4 sillimanite + 5 quartz as a geological thermometer in the Opinicon Lake region, Ontario. Contr. Mineral. Petrol. 33, 215–226.

Daubrée, M. A. (1859): Etudes et expériences synthétiques sur le metamorphisme et sur la formation des roches cristallines. Annales des mines, 5 sér., 6, 155–218 et 393–476.

Deer, W. A., Howie, R. A. and Zussman, J. (1962): Rock-Forming Minerals, Vol. 1–5, Longmans.

Dollase, W. A. and Hollister, L. S. (1969): X-ray evidence of ordering differences between sectors of a single staurolite crystal. Geol. Soc. Amer. Abstr. 1/7, 268–269.

Ernst, W. G. (1973): Interpretative Synthesis of metamorphism in the Alps. Geol. Soc. Amer. Bull. 84, 2053–2078.

Evans, B. W. (1965): Application of a reaction-rate method to the breakdown equilibria of muscovite and muscovite plus quartz. Amer. J. Sci. 263, 647–667.

Frey, M. (1969): Die Metamorphose des Keupers vom Tafeljura bis zum Lukmanier-Gebiet. Beitr. Geol. Karte Schweiz, N.F. 137, 160 p.

Friedländer, C. (1929): Der Chloritoid vom Crestlianderstobel. SMPM 9, 247–264.

Ganguly, J., and Newton, R. C. (1968): Thermal stability of chloritoid at high pressure and relatively high oxigen fugacity. J. Petrol. 9, 444–466.

Gibbs, G. V. (1966): The polymorphism of cordierite. I: The crystal structure of low cordierite. Amer. Mineral. 51, 1068–1087.

Goldschmidt, V. M. (1911): Die Kontaktmetamorphose im Kristianiagebiet. Oslo Vidensk. Skr. I. Math.-Nat. Kl. no. 11.

Gorbatschev, R. (1968): Distribution of elements between cordierite, biotite and garnet. N. Jb. Min. Abh. 110, 57–80.

Grünenfelder, M., Krebs, O. and Wenk, H. R. (1974): U-Pb ages of pelitic rocks in the Bergell area. (in preparation).

Gulson, B. L. (1973): Age relations in the Bergell region of the southeast Swiss Alps: With some geochemical comparisons. Eclogae geol. Helv. 66, 293–323.

Gulson, B. L. and Krogh, T. E. (1973): Old lead components in the young Bergell massif, south-east Swiss Alps. Contr. Mineral. Petrol. 40, 239–252.

Gyr, T. (1967): Geologische und petrographische Untersuchungen am Ostrande des Bergeller Massivs. Diss. ETH Zürich, 125 p.

Hänny, R. (1972): Das Migmatitgebiet der Valle Bodengo. Beitr. Geol. Karte Schweiz, N.F. 145, 1–109.

Hensen, B. J. and Green, D. H. (1971): Experimental study of the stability of cordierite and garnet in pelitic compositions at high pressures and temperatures. I. Compositions with excess aluminosilicate. Contr. Mineral. Petrol. 33, 309–330.

Hess, P. C. (1969): The metamorphic paragenesis of cordierite in pelitic rocks. Contr. Mineral. Petrol. 24, 191–207.

Hietanen, A. (1969): Distribution of Fe and Mg between garnet, staurolite and biotite

in aluminum-rich schists in various metamorphic zones north of the Idaho batholith. Amer. J. Sci. 267, 422–456.

HOLDAWAY, M. J. (1971): Stability of andalusite and the aluminum silicate phase diagram. Amer. J. Sci. 271, 97–131.

HOLST-PELLEKAN, W. VAN (1913): Geologie der Gebirgsgruppe des Piz Scopl. Diss. Univ. Zürich.

JÄGER, E. (1973): Die alpine Orogenese im Lichte der radiometrischen Altersbestimmungen. Eclogae geol. Helv. 66, 11–21.

IIYAMA, T. (1960): Recherches sur le rôle de l'eau dans la structure et le polymorphisme de la cordiérite. Bull. Soc. franç. Minér. Crist. 83, 155–178.

JUSTIN-VISENTIN, E. and ZANETTIN, B. (1968): Genesi di cornubianiti a staurolite-granato-andalusite-cordierite nell aureola di contatto dell'Adamello. Studi Trentini di Scienze Naturali 45, 224–245.

LANGER, K. and SCHREYER, W. (1969): Infrared and powder X-ray diffraction studies on the polymorphism of cordierite. Amer. Min. 54, 1442–1459.

LEAKE, B. E. (1960): Compilation of chemical analyses and physical constants of natural cordierites. Amer. Min. 45, 282–298.

LUTH, W. C., JAHN, R. H. and TUTTLE, O. F. (1964): The granite system at pressures of 4–10 kilobars. J. Geoph. Res. 69, 759–773.

MIYASHIRO, A. (1957): Cordierite-indialite relations. Amer. J. Sci. 255, 43–62.

— (1958): Regional metamorphism of the Gosaisyo-Takanuki district in the central Abukuma plateau. Univ. Tokyo J. Fac. Sci. sec. 2, 11, 219–272.

— (1973): Metamorphism and metamorphic belts. London.

MOTICSKA, P. (1970): Petrographie und Strukturanalyse des westlichen Bergeller Massivs und seines Rahmens. SMPM 50, 355–443.

NEWTON, R. C. (1972): An experimental determination of the high pressure stability limits of magnesian cordierite under wet and dry Conditions. J. Geol. 80, 398–420.

NIGGLI, E. (1960): Mineralzonen der alpinen Metamorphose in den Schweizer Alpen. Rep. Int. Geol. Congr. XXI Session Pt. XIII, 132–138.

NIGGLI, E. und NIGGLI, C. R. (1965): Karten der Verbreitung einiger Mineralien der alpidischen Metamorphose in den Schweizer Alpen (Stilpnomelan, Alkali-Amphibol, Chloritoid, Staurolith, Disthen, Sillimanit). Eclogae geol. Helv. 58, 335–368.

RAMBERG, H. (1967): Gravity, deformation and the earth's crust; as studied by centrifuged models. London, 214 p.

RAYMOND, K. N. (1972): The application of constraints to derivatives in least squares refinement. Acta Cryst. A 28, 163–166.

REPOSSI, E. (1916): La bassa Valle della Mera. Studi petrografici e geologici II. Mem. Soc. Ital. Sci. Nat. Milano 8, 186 p.

RICHARDSON, S. W. (1968): Staurolite stability in a part of the system Fe-Al-Si-O-H. J. Petrol. 9, 467–489.

RICHARDSON, S. W., GILBERT, M. C. and BELL, P. M. (1969): Experimental determination of kyanite-andalusite and andalusite-sillimanite equilibria; the aluminum silicate triple point. Amer. J. Sci. 267, 259–272.

ROBIE, R. A., and WALDBAUM, D. A. (1968): Thermodynamic properties of minerals and related substances at 298.15° K (25.0° C) and one atmosphere (1.013 Bars) pressure and at higher temperatures. US Geol. Survey Bull. 1259, 256 p.

ROSENBUSCH, H. (1877): Die Steiger Schiefer und ihre Kontaktzone an den Graniten von Barr-Andlau und Hohwald. Abh. geol. Spezialkarte Elsass-Lothr. Bd. I, H. 11.

SAXENA, S. K., and GHOSE, S. (1971): Mg^{2+}-Fe^{2+} Order-Disorder and the Thermodynamics of the Orthopyroxene Crystalline Solution. Amer. Mineral. 56, 532–559.

Schreyer, W. (1965): Zur Stabilität des Ferrocordierites. Contr. Min. Petr. 11, 297–322.
— (1966): Synthetische und natürliche Cordierite III. Polymorphiebeziehungen. N. Jb. Mineral. Abh. 105, 211–244.
Schreyer, W. and Yoder, H. S. (1964): The system Mg-cordierite-H_2O and related rocks. N. Jb. Mineral., Abh. 101, 271–342.
Schreyer, W. and Seifert, F. (1969): Compatibility relations of the aluminum silicates in the systems MgO-Al_2O_3-SiO_2-H_2O and K_2O-MgO-Al_2O_3-SiO_2-H_2O at high pressures. Amer. J. Sci. 267, 371–388.
Schwander, H. und Stern, W. (1969): Zur Analyse von Cordierit. SMPM 49, 585–595.
Seifert, F. (1970): Low temperature compatibility relations of cordierite in haplopelites of the system K_2O-MgO-Al_2O_3-SiO_2-H_2O. J. Petrology 11, 73–99.
Tilley, C. E. (1925): Metamorphic zones in the southern highlands of Scotland. Geol. Soc. London Quart. J. 81, 100–112.
Thompson, J. B. (1957): The graphical analysis of mineral assemblages in pelitic schists. Amer. Minral. 42, 842–858.
Trommsdorff, V. (1966): Progressive Metamorphose kieseliger Karbonatgesteine in den Zentralalpen zwischen Bernina und Simplon. SMPM 46, 431–460.
Van der Plas, L., Hügi, Th., Mladeck, M. H. und Niggli, E. (1958): Chloritoid vom Hennensädel südlich Vals (nördliche Adula). SMPM 38, 237–246.
Virgo, D. and Hafner, S. S. (1969): Fe^{+2}, Mg Order-Disorder in Heated Orthopyroxenes. Mineral. Soc. Amer. Spec. Pap. 2, 67–81.
Weber, W. (1966): Zur Geologie zwischen Chiavenna und Mesocco. Diss. ETH Zürich, 248 p.
Wenk, E. (1956): Die lepontinische Gneisregion und die jungen Granite der Valle della Mera. Eclogae geol. Helv. 49, 251–265.
— (1962): Plagioklas als Indexmineral in den Zentralalpen. SMPM 35, 311–319.
— (1968): Cordierit in V. Verzasca. SMPM 48, 455–458.
— (1973): Cordierit-Drilling aus Hornfelsgneiss der Albigna (Bergell). SMPM 53, 31–32.
Wenk, E. and Keller, F. (1969): Isograde in Amphibolitserien der Zentralalpen. SMPM 49, 157–198.
Wenk, H.-R. (1967): Triklinität der Alkalifeldspäte in lepontinischen Gneissen. SMPM 47, 129–146.
— (1970): Geologische Beobachtungen im Bergell. 1. Gedanken zur Geologie des Bergeller Granits. Rückblick und Ausblick. SMPM 50, 321–349.
— (1973): The structure of the Bergell Alps. Eclogae geol. Helv. 66, 255–291.
— (1974): Two episodes of high-grade metamorphism in the northern Bergell Alps. SMPM, 54, 555–565.
Wenk, H.-R. and Raymond, K. N. (1973): Four new structure refinements of olivine. Z. Krist. 137, 86–105.
Wood, B. J. (1973): Fe^{2+}-Mg^{2+} partition between coexisting cordierite and garnet – a discussion of the experimental data. Contr. Mineral. Petrol. 40, 253–258.
Wood, B. J. and Banno, S. (1973): Garnet-Orthopyroxene and Orthopyroxene-Clinopyroxene Relationships in Simple and Complex Systems. Contr. Mineral. Petrol. 42, 109–124.
Zachariasen, W. H. (1968): Experimental tests of the general formula for the integrated intensity of a real crystal. Acta Cryst. A 24, 212–216.

Manuscript received February 4, 1974.